US Army Corps
of Engineers
Construction Engineering
Research Laboratory

CERL Technical Report 99/85
October 1999

Electrochemical Reduction of Nitro-Aromatic Compounds

Product Studies and Mathematical Modeling

Devakumaran Meenakshisundaram, Manish Mehta, Simo Pehkonen, and Stephen W. Maloney

Nitro-aromatics 2,4,6-trinitrotoluene (TNT), 2,4-dinitrotoluene (DNT) and hexa-hydro-1,3,5-trinitro-triazine (RDX) are the major constituents of wastewaters discharged from propellant and explosive manufacturing units and munitions load, assembly, and pack operations. More than 1,200 current and former U.S. Department of Defense and Department of Energy facilities have problems with explosive contamination.

The objective of this project was to study the electrochemical degradation of nitro-aromatic compounds under various conditions to enable the formulation of a mathematical model and to design a plug flow reactor for the same. The first set of experiments evaluated the effect applied current, stir rate of the reactant solution, and surface area of the electrode has on the degradation of DNT. The second phase of experiments was to identify the products being formed as well as selected intermediates. The third phase of experiments involved kinetic and certain mass transfer experiments to aid in setting up the mathematical model. After initial work with DNT in pure water, the study was expanded to evaluate the electrochemical reduction of TNT, DNT (in water-ethanol mixture), and RDX under different conditions to evaluate the optimal degradation conditions and to propose the design of a plug flow reactor based on those conditions. Controlled experiments based on single solute nitro-aromatics were carried out initially to ascertain the degradation of these chemicals by electrochemical means and to establish the different water-quality variables and reactor parameters. The fourth phase of experiments identified the products and some selected intermediates during the degradation of TNT and DNT. The fifth phase of study aimed at establishing a correlation between theory and experimental results by explaining the observed kinetic data in terms of the possible mechanisms limiting the transformation rates in the electrochemical systems. Also, experiments involving improved hydrodynamics to overcome mass transfer limitations (if observed) were carried out. The final stage of the project involved the design proposal of a treatment assembly using a plug flow type reactor for the electrochemical degradation of nitro-aromatics in munitions wastewaters.

US Army Corps
of Engineers
Construction Engineering
Research Laboratory

CERL Technical Report 99/85
October 1999

Electrochemical Reduction of Nitro-Aromatic Compounds

Product Studies and Mathematical Modeling

Devakumaran Meenakshisundaram, Manish Mehta, Simo Pehkonen, and Stephen W. Maloney

Foreword

This study was conducted for Headquarters, U.S. Army Corps of Engineers (HQUSACE) under Project 4A162720D048, "Industrial Operations Pollution Control Technology"; Work Units U08 and U09, "Electrochemical Reduction of Aromatic Compounds." The technical monitor was Chris Vercautren, Industrial Operations Command, Rock Island Arsenal, IL.

The work was performed by the Environmental Processes Branch (CN-E) of the Installations Division (CN), U.S. Army Construction Engineering Research Laboratory (CERL). The study was performed, in part, by the University of Cincinnati, Cincinnati, Ohio, under contract to CN-E. Simo Pehkonen is an assistant professor and Devakumaran Meenakshisundaram and Manish Mehta were graduate students with the Department of Civil and Environmental Engineering at the University of Cincinnati. The CERL principal investigator was Stephen W. Maloney. L. Jerome Benson is Chief, CN-E, and Dr. John T. Bandy is Division Chief, CN. The technical editor was Linda L. Wheatley, Information Technology Laboratory.

Dr. Michael J. O'Connor is Director of CERL.

Contents

List of Figures and Tables

Figures

Tables

1 Introduction

Background

Nitro-aromatics 2,4,6-trinitrotoluene (TNT), 2,4-dinitrotoluene (DNT), and hexahydro-1,3,5-trinitro-triazine (RDX) are the major constituents of wastewaters discharged from propellant and explosive manufacturing units and munitions load, assembly, and pack operations. DNT enters the wastestream during propellant production, whereas TNT and RDX enter wastestreams during munitions loading and demilitarization. Wastewater contaminated with TNT and RDX is referred to as pinkwater, due to its characteristic color. The high explosive TNT constitutes a significant component of a widespread munitions contamination problem that exists at many current and former U.S. Department of Defense (DOD) and U.S. Department of Energy (DOE) facilities. More than 1,200 sites have explosive contamination (Tri-Service 1992). At many of these sites, the contamination has been found in the groundwater.

TNT is the most common contaminant found in both soil and water samples (Jenkins and Walsh 1993). Most process waters found at the contaminated sites are pinkwaters that were generated by demilitarization operations conducted in the 1970s. DNT has also been found frequently at munitions-contaminated sites. Both TNT and DNT are listed as priority pollutants by the U.S. Environmental Protection Agency (EPA) because of their toxicological hazards. The LD_{50} value of DNT in rats is 268 mg/kg (Sax and Lewis 1989). From a toxicological standpoint, the identification of the products from the transformation of DNT, and for that matter any nitro-aromatic compound, is essential as the products may turn out to be more hazardous.

Trinitrotoluene can have three structural isomers: 2,3,5 TNT, 2,4,6 TNT, and 2,4,5 TNT. The symmetrical 2,4,6-trinitrotoluene is the most commonly found form of the three and henceforth in this report the acronym TNT will be used to refer to 2,4,6-trinitrotoluene only. TNT is still the most widely used military explosive because of its low melting point (80.1 °C), stability, low sensitivity to impact, and relatively safe methods of manufacture. TNT has been classified as a high explosive (Kline 1990) and used as a military explosive in bombs and grenades, generally in binary mixtures with a primary explosive to trigger the main explosion. It is also used as an industrial explosive for deep water and

underwater blasting. TNT is prepared by the nitration of toluene with a mixture of nitric acid and sulfuric acid (Fisher and Taylor 1983). It is released into the waste stream during manufacturing, loading, assembling, and packing operations.

DNT has six isomers. The 2,4- and 2,6- isomers are the most important because they are the greatest quantities produced anthropogenically (Beard and Noe 1981). DNT is prepared by the nitration of toluene and nitrotoluene in the presence of nitric and sulfuric acids. One of the major uses of DNT is as an intermediate in the manufacture of toluene diisocyanate, which is then used in the production of polyurethane foams. Another major use of DNT is as an ingredient in military and commercial explosives; the purified form of 2,4-DNT is used in smokeless powders (Bausum, Mitchell, and Major 1992).

RDX, or cyclonite as it is commonly referred to, is an explosive used extensively as a propellant for propelling artillery shells and as an explosive in projectiles. It is so used because it offers higher energy, higher density, and lower flame temperatures. It is often used in binary mixtures with TNT. It finds its way into the munition wastewaters during manufacturing and blending operations.

Objectives

The objectives of this project were to study: (1) the kinetics of electrochemical degradation of DNT (with and without ethanol), TNT, and RDX, (2) the mechanisms of electrochemical reduction of 2,4 DNT and 2,4,6 TNT from the point of view of product studies, (3) the effect of stirring rate, pH, current density and dissolved oxygen on the degradation of the nitro-aromatic, (4) theoretical explanation of the observed kinetic results and the mass transfer limitations encountered in the system, and (5) a method to overcome the mass transfer limitations, and the final setup of the treatment assembly to carry out the degradation of nitro-aromatics using electrochemistry.

Approach

Degradation of the nitro-aromatics was studied at the bench-scale in an electrochemical reactor, which was fabricated at the beginning of the project. The rate of degradation was measured under various experimental conditions, including the surface area of electrodes, stirring rate, current settings, pH, and the level of dissolved oxygen. The by-products of degradation were identified by gas chromatography/mass spectometry (GC/MS) for DNT and by high performance

liquid chromatography (HPLC) for TNT. A mass balance for the products was obtained under a variety of experimental conditions in both the aqueous and solid phases. The degradation behavior was then assessed in light of the experimental results obtained and conclusions were drawn from the data in order to address the objectives of the research.

Scope

The techniques described in this report apply to Army industrial activities. The agencies responsible for development and treatment of Army-specific explosives and other aqueous wastestreams will benefit from the information presented herein. The goals of developing and understanding new technology potentially applicable to nitrated explosives are addressed. The pathways of treatment and by-products identified will provide guidance tools for process scale-up and pilot testing.

Mode of Technology Transfer

It is anticipated that the findings and recommendations in this report will be used as a foundation for developing and testing a pilot-scale system based on electrochemical reduction of munitions wastewaters. The results will be presented at Army conferences and scientific meetings to further the application of this new method for treatment of synthetic organic chemicals that are resistant to oxidative degradation.

2 Literature Review

An explosives contamination problem has been found in the ground water at many DOE and DOD sites. TNT is the most common contaminant found in both soil and water samples. Other nitro-aromatics, especially DNT, have also frequently been found at munitions-contaminated sites. Both TNT and DNT are listed by the EPA as priority pollutants because of their toxicological properties. From a toxicological standpoint, the identification of the products from transformations of nitro-aromatic compounds is essential because the products are often more hazardous than the starting compounds.

Biological Pathways

Biological transformations mainly occur through oxidation and reduction. Oxidation occurs when oxygen is the reactant and oxygenase or peroxidase enzymes mediate the cleavage of the aromatic ring. Reduction is the more common mechanism and takes place when the nitro-aromatic compound is reduced to arylamines by a mechanism of hydrolytic deamination, acetylation, reductive deamination, and cyclization.

It was found that *Pseudomonas* species degraded both DNT and TNT aerobically with supplemental glucose as a carbon source (Schackmann and Muller 1991; Parrish 1977). Reduction of the nitro groups took place only at the para positions and proceeded through the hydroxylamino-nitrotoluene to the amino-nitrotoluene. McCormick, Cornell, and Kaplan (1978) identified the biotransformation products during the conversion of DNT to 2,4-diaminotoluene (DAT). These pathways are shown in Figure 1. Haidour and Ramos (1996) observed 2-hydroxylamino-4,6-dinitrotoluene, 4-hydroxylamino-2,6-dinitrotoluene, 4-amino-2,6-dinitrotoluene, 2-amino-4,6-dinitrotoluene, and 2,4-diamino-nitrotoluene as the products of degradation of TNT with *Pseudomonas* sp. Boopathy, Wilson, and Kulpa (1993) reported the anaerobic degradation of TNT under different electron accepting conditions by a soil bacterial consortium. Hughes et al. (1998) demonstrated the ability of *Clostridium acetobutylicum* to reduce TNT to 2,4-dihydroxylamino-6-nitrotoluene and then to phenolic products via the Bamberger rearrangement. The transformation pathway is shown in Figure 2.

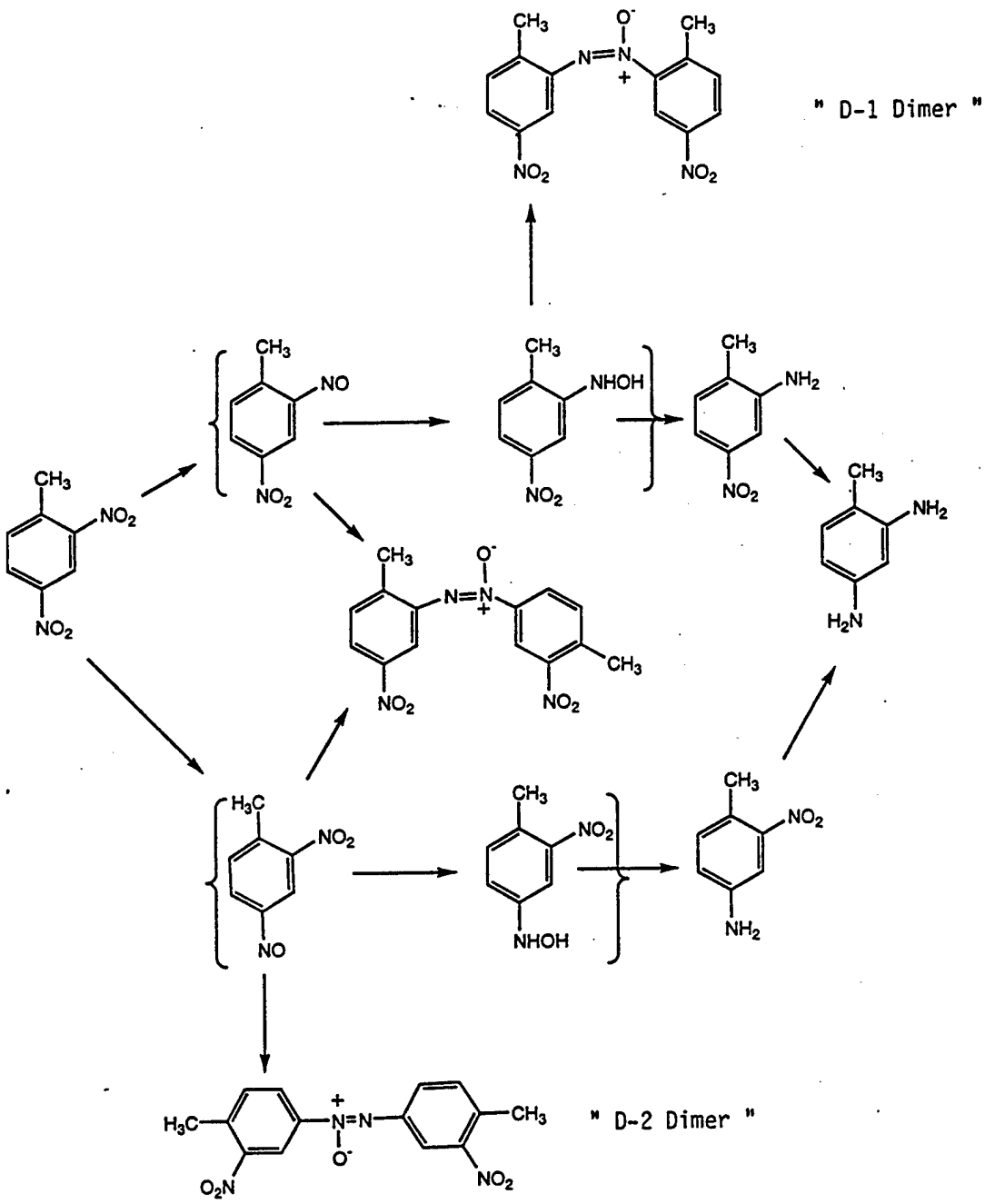

(Source: McCormick, Cornell, and Kaplan 1978. Used with permission of the American Society of Microbiology.)

Figure 1. Reaction pathway for the biotransformation of DNT to DAT.

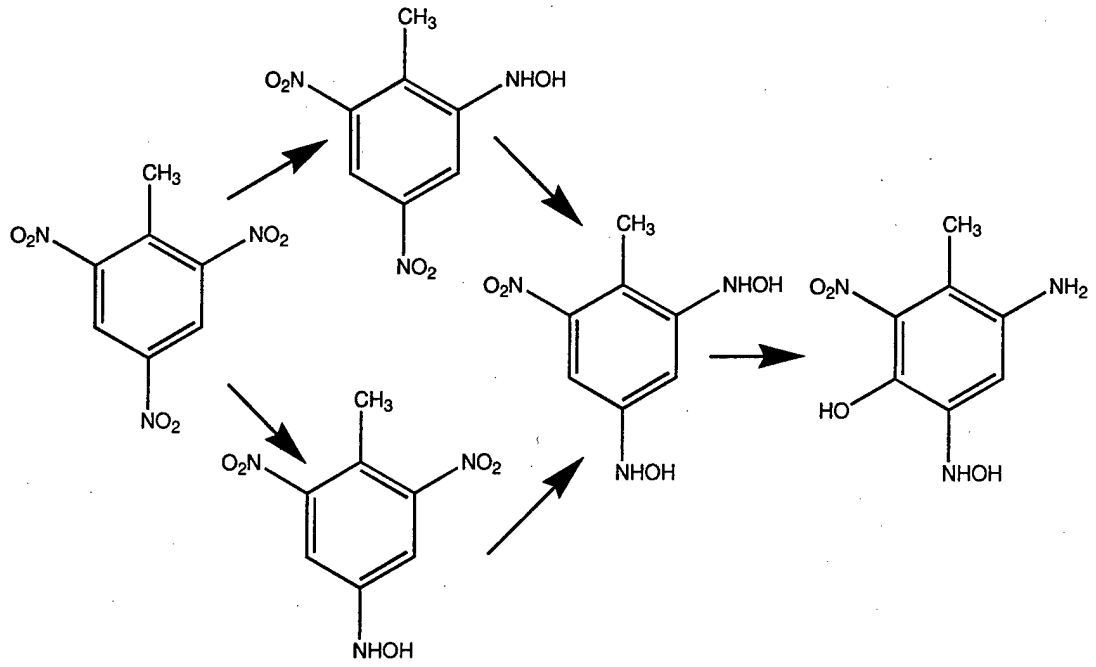

(Source: Reprinted with permission from Hughes et al. 1998. Copyright 1998 American Chemical Society.)

Figure 2. Pathway of TNT transformation observed in *C. acetobutylicum* crude cell extracts.

A fungi *Mucrosporium* aerobically dégraded DNT. The identified biotransformation intermediates include: 2-amino-4-nitrotoluene, 4-amino-2-nitrotoluene, 4,4'-dinitro-2,2'-azoxytoluene, 2,2'-dinitro-4,4'-azoxytoluene, and 4-acetamido-2-nitrotoluene. A third azoxy compound, 2,4'-dinitro-2,4'-azoxytoluene or 4,2'-dinitro-4,2'-azoxytoluene, was isolated but not yet identified conclusively. An anaerobic municipal activated sludge system with benzene added as a carbon source resulted in successful degradation of DNT.

Noguera and Freedman (1996) showed that a *Pseudomonas aeruginosa* strain was capable of reduction and acetylation of DNT. Under anoxic conditions, the main products were 2-amino-4-nitrotoluene and 4-acetamide-2-nitrotoluene. 4-amino-2-nitrotoluene was very rapidly acetylated to 4-acetamide-2-nitrotoluene, and 2-amino-4-nitrotoluene was very slowly degraded to DAT and 2-acetamide-4-nitrotoluene.

Spanggord et al. (1991) showed the ability to completely mineralize DNT by an oxidative pathway with a *Pseudomonas* species using DNT as the sole carbon source. The nitro groups were removed without reduction to amines. Dioxygenase attack was responsible for the nitro group reduction and a subsequent release as nitrite. Valli et al. (1992) was able to degrade DNT by the

lignin-degrading fungus *Phanerochaete chrysosporium*. This fungus contained two peroxidases, which are responsible for the complete mineralization of DNT to CO_2 in nitrogen-limiting cultures. The treatment of DNT using a two-stage system has also been shown to completely mineralize DNT with 2-amino-4-nitrotoluene and 4-amino-2-nitrotoluene as intermediates (Berchtold et al. 1995).

Biotransformation of RDX has been observed by a number of researchers. Young et al. (1997) found a bacterial consortium in horse manure capable of degrading RDX at the rate of 0.022 L/gram cells per hour. Most of the research in the biological degradation of RDX has been carried out under anaerobic conditions.

Kitts et al. (1994) isolated three different genera of bacteria, which were able to degrade RDX. The most effective degrader of these three isolates was identified as *Morganella morganii*. One pathway for the biotransformation of RDX is a stepwise reduction of each of RDX's three nitro groups to form nitroso groups as shown in Figure 3.

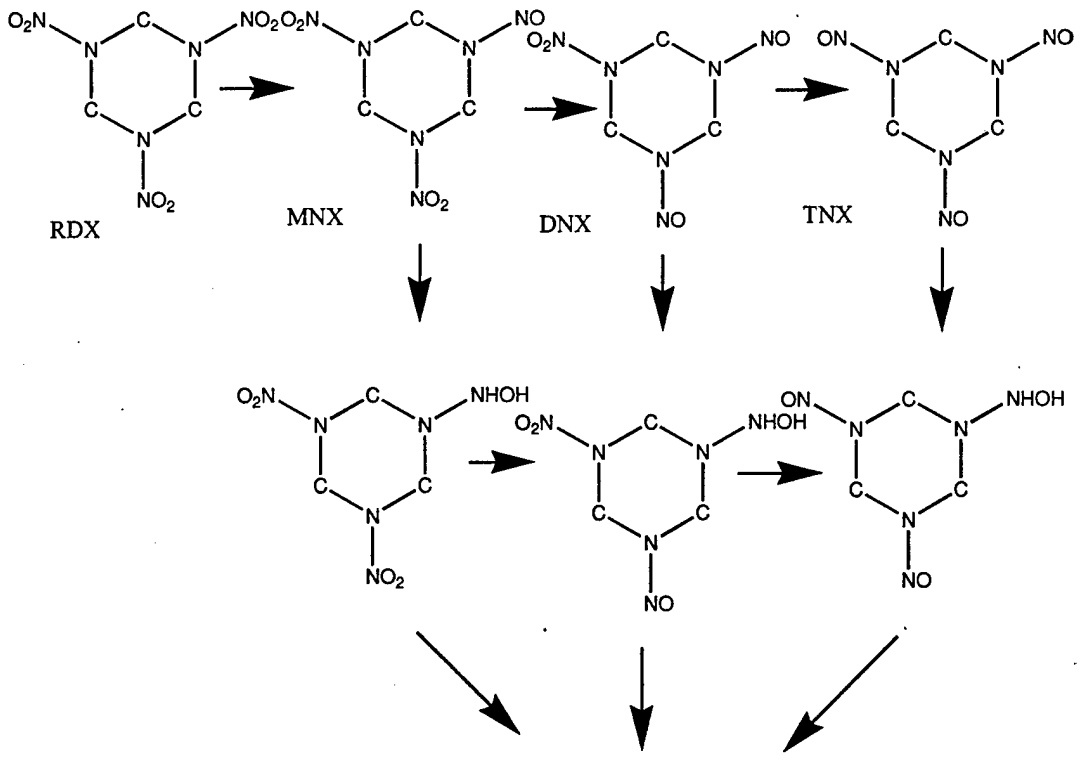

(Source: McCormick et al. 1981; Kitts et al. 1994. Used with permission of the American Society for Microbiology.)

Figure 3. Stepwise reduction of RDX through reduction of nitroso groups.

Chemical Pathways

The most common method for transformation of nitro-aromatics at present is incineration. However, while incineration has been demonstrated to be an effective technology, issues such as safety, noise, air emissions, costs, regulatory requirements, etc., have motivated research in alternative treatment technologies. The adsorption of TNT and DNT (Ho and Daw 1988) on activated carbon was one of the most common treatment technologies used by the military ammunition plants. This technology is effective at removing a wide variety of explosive contaminants from water, but is nondestructive and expensive to operate. Moreover, after the carbon is exhausted, it has to be incinerated or disposed of into a hazardous waste disposal site. The disposal of used carbon is very costly.

The photochemical degradation of TNT has been extensively researched. It has been considered both as a primary treatment technology and as a pretreatment to bioremediation. TNT strongly absorbs UV radiation between 200 and 280 nm. Exposure of TNT to sunlight or near UV radiation results in the rapid conversion of TNT into a variety of aromatic photolysis products including the nitroamines and azoxy dimers, which are also found in biodegradation.

It was demonstrated by Schmelling and Gray (1995) that TiO_2 photocatalysis using near UV radiation may be highly effective in the remediation of TNT contaminated waters. Photocatalytic transformation of TNT was shown to include both oxidative and reductive steps. Trinitrobenzoic acid, trinitrobenzene, and trinitrophenol were observed as oxidative intermediate species, and 3,5-dinitroaniline was identified as a stable reduction product. These two pathways are shown in Figures 4 and 5.

Other technologies investigated in application to TNT remediation are: clay/resin adsorption, ionizing radiation, supercritical oxidation, UV-ozone and wet-air oxidation.

The other major chemical method, which is widely reported in scientific literature, is the catalytic hydrogenation of DNT over a Pd/C catalyst. Palladium-catalyzed hydrogenation has been found to completely reduce DNT to DAT (Terpko and Heck 1980; Janssen et al. 1990). For DNT, the less hindered or para-position was reduced with a very high yield (92 percent). However, for the four other 2,4-dinitro-aromatic compounds tested (with -OH, $-OCH_3$, $-NH_2$, and $-NHCOCH_3$ groups instead of $-CH_3$), the more hindered or ortho-position was reduced. Janssen et al. (1990) found two parallel reaction pathways for the formation of DAT from DNT in a palladium catalyzed hydrogenation reaction. There were three stable reaction intermediates: 4-hydroxylamino-2-nitro-

toluene, 4-amino-2-nitrotoluene, and 2-amino-4-nitrotoluene. Very low concentrations of 4-hydroxylamino-2-nitrotoluene were found. This suggested that the nitro group in the ortho position was converted almost directly to the amino group.

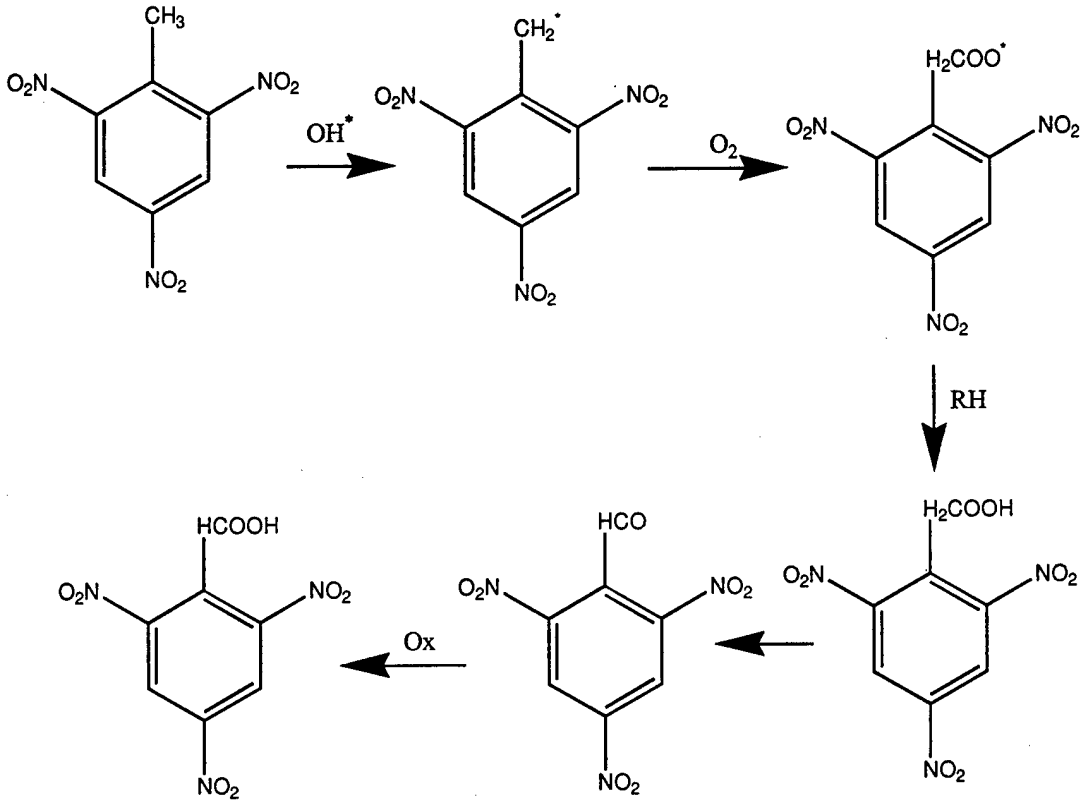

(Source: Schmelling and Gray 1995. Used with permission from Elsevier Science.)

Figure 4. Reaction pathway for the initial oxidative transformation of TNT under photocatalytic conditions.

Nitro-aromatic compounds undergo reductive transformations to aromatic amines. The reduction of nitro-aromatics occurred through a series of electron-transfer reactions and protonations with nitroso compounds and hydroxylamines as highly reactive intermediates. Barrows et al. (1996) found that the location of the first nitro group reduced was influenced by the regioselectivity for substituted polynitroaromatic compounds. The regioselectivity was important in the first proton transfer to the radical anion that was created after the initial one electron reduction of the starting compound. Localization of the charge in the initial radical anion influenced the site of protonation. Of the 10 polynitroaromatic compounds studied, all but 2 showed localization of the radical ion on the nitro group in the ortho position. The two with the localized radical ion in the para-position were DNT and TNT. DNT showed an 88 to 92 percent regioselectivity for the para-position and TNT showed 100 percent regioselectivity.

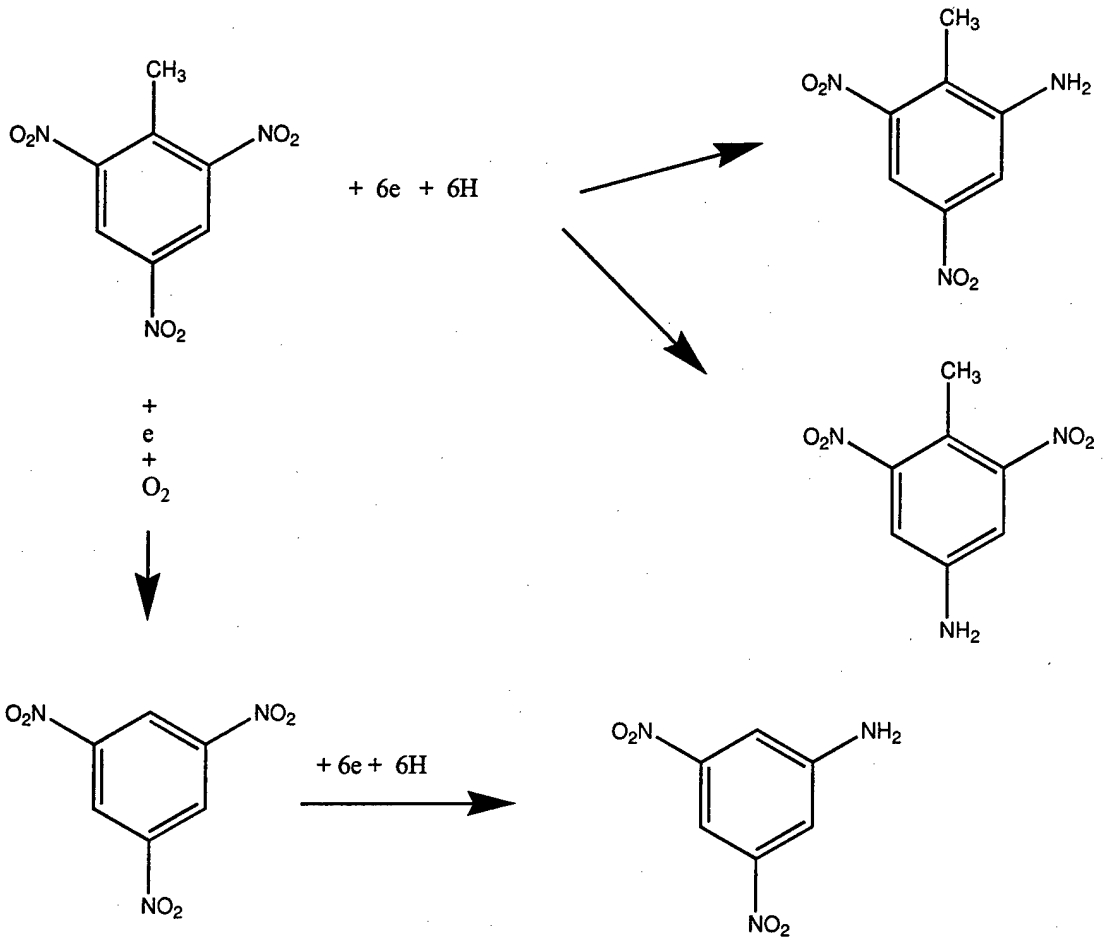

(Source: Reprinted with permission from Schmelling, Gray, and Kamat 1996. Copyright 1996 American Chemical Society.)

Figure 5. Photochemical transformation observed during the reductive degradation of TNT.

Electrochemical Pathways

Many studies have been carried out on the electrochemistry of nitro-organics. The nitrogen in the nitro group is already at a high oxidation state, +3. DNT has no known anodic chemistry since it is extremely difficult to remove an electron (Fry 1982). The nitrosobenzene intermediate was rarely observed (Shindo and Nishihara 1989; Martigny and Simonet 1983), although evidence for its formation has been observed by the formation of the azoxy and azobenzene dimers (Laviron and Vallat 1973). For the reduction of nitro-aromatic compounds by zero-valent Fe under anaerobic conditions, no azo or azoxy dimers were found with the Fe^0 reduction.

Electrochemical reduction of nitrated organic compounds has been studied in nonaqueous solvents from the viewpoint of methods for synthesis of organic chemicals. Evans and coworkers have studied the reduction of 1,1-dinitrocyclohexane (Bowyer and Evans 1988; Ruhl et al. 1991) and several nitroalkanes (Ruhl, Evans, and Neta 1992) in dimethylformamide. They demonstrated that these protective nitro groups could be reduced by electrochemistry. In a related study (Kopilov and Evans 1990), it was found that dehalogenation can occur when electrochemical reduction is applied to a-haloacetanilides in alcohol and acetonitrile. These same groups (nitro- and halo-) protect the compounds from biological attack. These studies in organic solvents suggest that the conversion may also be possible by the use of electrodes in water, for the purpose of opening up the contaminant to conventional biodegradation.

Electrochemical Engineering

Electrochemical engineering is the knowledge required to either design and run an industrial plant that includes an electrolytic stage for the production of chemicals or to produce an electrolytic device for the generation of electricity. The former involves the use of electricity for the production of chemicals, and the latter involves the use of chemicals for the production of electricity. Figure 6 shows a general schematic for the design of electrochemical reactors. The first step is a reaction model, which tells us how current density varies as a function of the kinetic and mass transfer elements. To determine the dependence of current density on electrode potential, kinetic constants from polarization and preparative runs have to be obtained. In addition, mass transfer coefficients for the laboratory cell used in these experiments should be available.

A reactor model is developed to provide such parameters as the required electrode area as a function of process variables (e.g., current density and conversion). To do this, modeling is begun by selecting a notional industrial cell configuration. Again, mass transfer data for the selected reactor should be available. By combining this reactor model with models for associated unit processes, one can arrive at a process model. Using cost analysis along with the process model enables optimization of the process and yields process specifications for the cell. If this turns out to be satisfactory, a mechanical design is undertaken; if not, a different cell geometry is selected and a new reactor model developed.

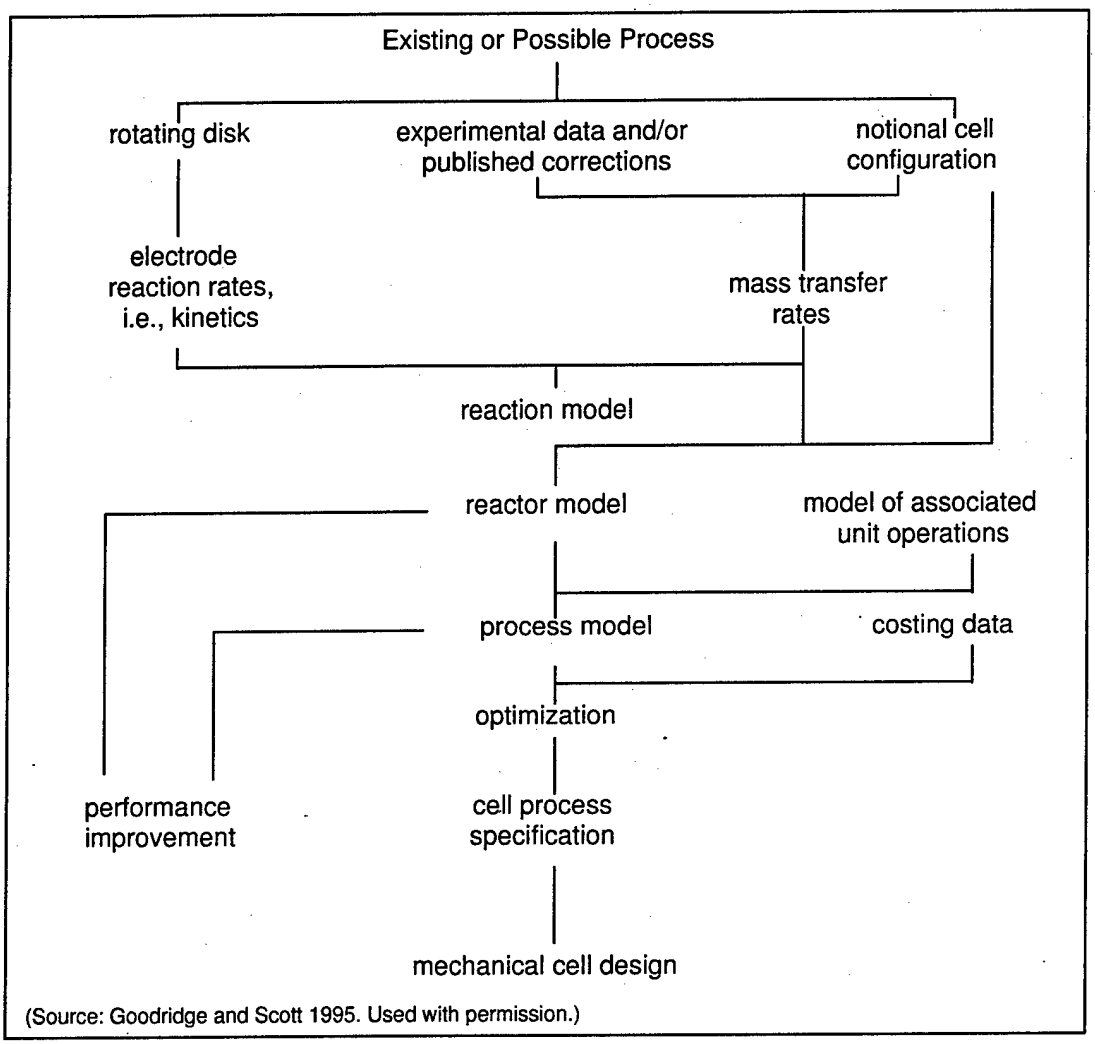

Figure 6. Scheme for the design of electrolytic reactors.

Fundamentals of Electrochemical Processes

Figure 7 shows the region at the interface between an electrode and an electrolyte. The potentials in the electrode and adjacent to the interface are denoted E_m and E_s. Their difference is referred to as the electrode potential, E':

$$E' = E_m - E_s \qquad \text{(Eq 1)}$$

At a cathode, positive current flows from the electrolyte to the electrode. Therefore, by the above definition, E' for cathode tends to be negative, and it is positive for an anode. If the electrode potential E' is kept constant and the area of the electrode is doubled, the current passing between the electrode and electrolyte is

also doubled (i.e., the current supported by an electrode is proportional to its area). The current supported by unit area of an electrode is referred to as the current density (i).

Information about electrode reactions can often be obtained from plotting i as a function of potential. A polarization curve is a plot of ln [i] against η, where η (i.e., overpotential) is defined as:

$$\eta = E' - E \qquad \text{(Eq 2)}$$

where E is the electrode potential when no current is flowing. An example of such a curve is shown in Figure 8.

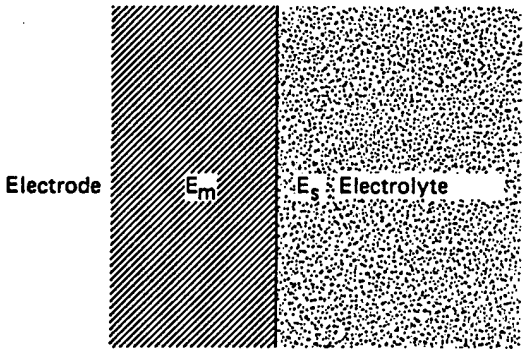

(Source: Goodridge and Scott 1995. Used with permission.)

Figure 7. Region near an electrode interface.

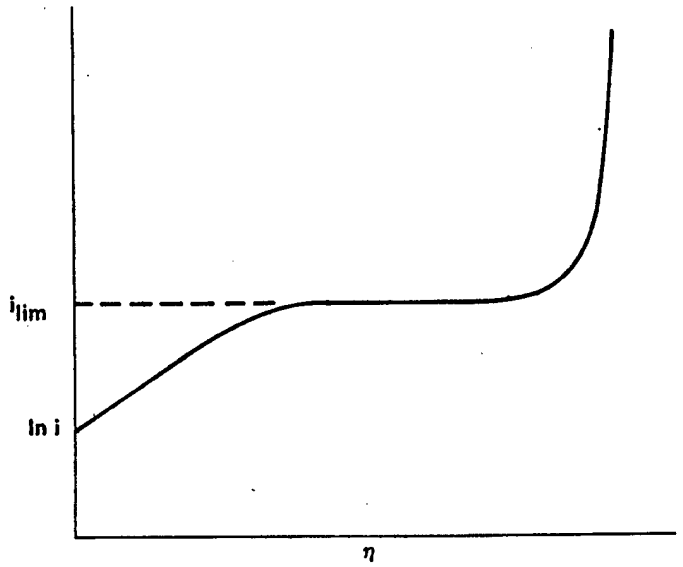

(Source: Goodridge and Scott 1995. Used with permission.)

Figure 8. Idealized polarization curve.

Defining the rate of reaction, r_A, as the rate of conversion of A per unit time per unit area of electrode, it follows from Faraday's law that:

$$r_A = ai/nF \quad \text{(Eq 3)}$$

$$i = (nFr_A)/a \quad \text{(Eq 4)}$$

where a is the stoichiometric coefficient of the reactant A. The current density for an electrochemical reaction is therefore equivalent to the rate of the reaction. The initial linear rise in current density in Figure 8 corresponds to conditions when the limiting step is the rate of charge transfer. The horizontal portion, where the current density becomes independent of the overpotential (η), represents the situation when mass transfer is rate controlling. This current (represented by i_{lim}) is known as the limiting current density. The further increase in current density beyond the plateau is due to the starting of another reaction.

Consider a process for the formation of product B where two simultaneous cathodic reactions are occurring:

$$A + ne^- \rightarrow B \quad \text{(Eq 5)}$$

and

$$2H^+ + 2e^- \rightarrow H_2 \quad \text{(Eq 6)}$$

The number of kmols of B formed per unit electrode area (nm_B) will be given according to:

$$nm_B = i_B\, t/F \quad \text{(Eq 7)}$$

Similarly, $2m_H$ (the number of kmols of hydrogen) will be:

$$2m_H = i_H\, t/F \quad \text{(Eq 8)}$$

where i_B and i_H are the partial current densities for Equations 5 and 6, respectively, and

$$i = i_B + i_H \quad \text{(Eq 9)}$$

where i is the current density for the whole process.

Current efficiency (C.E), sometimes called Faradaic yield of the process, is defined by:

$$C.E = nm_B/(nm_B + 2m_H) = i_B/i \quad \text{(Eq 10)}$$

Another important concept in electrochemistry is that of the double layer. Consider the following elementary reaction:

$$Ag^+ + e^- = Ag \quad \text{(Eq 11)}$$

by which silver is deposited or dissolved electrolytically.

If a silver electrode is immersed in an aqueous solution of a silver salt and rendered cathodic, it will contain an excess of electrons (Figure 9). These electrons and the silver cations existing in the surrounding electrolyte will be mutually attracted, and the anions in the electrolyte will be repelled. As a result, an excess of positive charge will occur in the region adjacent to the electrode. This region consists of two entities, a compact layer (the Helmholtz layer) and a diffuse layer. The compact layer is a few angstroms thick, while the diffuse layer is up to several hundred angstroms, depending on the potential of the electrode and the concentration of ionic species at the electrode.

Solvent molecules occupy the region between the ions in the compact layer and the electrode surface. If the solvent is water, the layer of solvent molecules is thought to be two molecules deep, with the layer nearer the electrode tending to be oriented so that the positive end of the dipoles point toward the electrode. This tendency increases as the electrode potential is made more negative. Intermingled with the solvent molecules may be other species, particularly anions, which may be specifically adsorbed on the electrode surface. Such adsorption requires displacement of the solvent molecules. The adsorption of anions creates a layer of charged species, which is closer to the electrode surface than the compact surface just described. The respective charges are located at the outer Helmholtz plane (xH in Figure 9) and the inner Helmholtz plane for the adsorbed species. Figure 9 also shows how E_s, the potential in the electrolyte, varies as a function of distance from the electrode. Although the cell voltage V^c has no fundamental theoretical significance affecting the electrode reaction, it is of great practical importance because electricity costs are directly proportional to it.

To minimize the cell voltage for a given current density, the following steps are taken:

1. Electrode materials are selected that minimize the electrode potential required for the desired reaction.

2. Distance between anode and cathode is kept at a minimum.

3. Conductivities of the anolyte and the catholyte are maximized.

4. A diaphragm is selected that produces the minimum voltage drop. If possible, the diaphragm is disposed of.

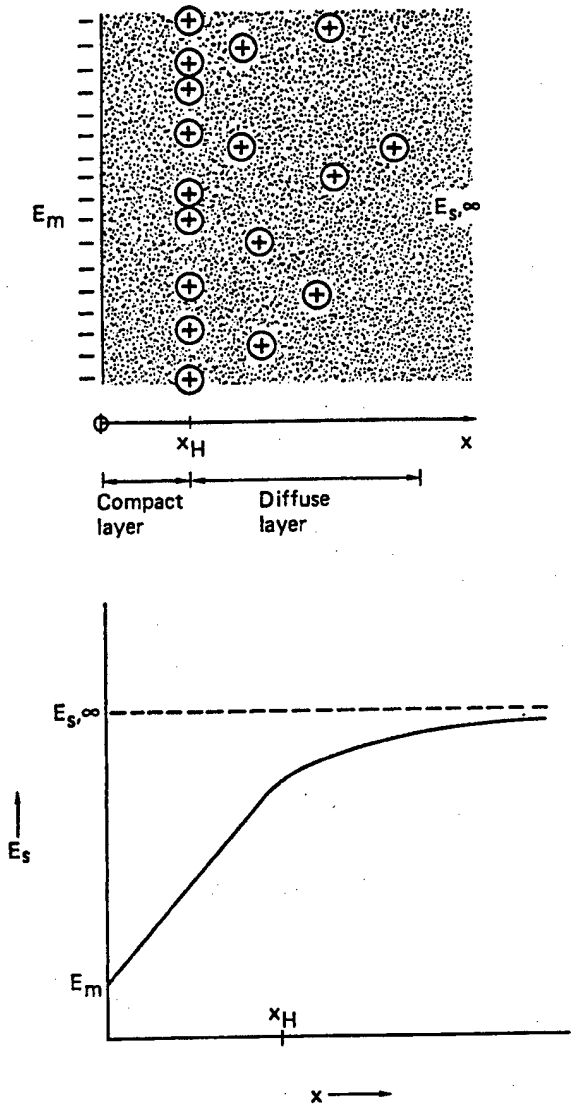

(Source: Goodridge and Scott 1995. Used with permission.)

Figure 9. Simple model of the electrical double layer and the resultant potential profile.

Aspects of Mass Transfer

The formation of the reaction model depends on knowing the rate at which the reactants arrive at the electrode surface from the bulk of the electrolyte and the rate at which the products formed by reactions disappear back into the bulk of the electrolyte.

The transfer of a solute O through a liquid can be affected by three mechanisms:

- molecular diffusion under the influence of a concentration gradient
- migration of a charged species under the influence of a potential or electric field
- eddy diffusion due to a turbulent regime.

Figure 10 gives the concentration profile near the electrode surface for a fully developed turbulent flow. There are three regions: a near horizontal portion corresponding to the fully mixed turbulent bulk, a linear decrease occurring in the laminar sublayer, and a curved portion connecting the two.

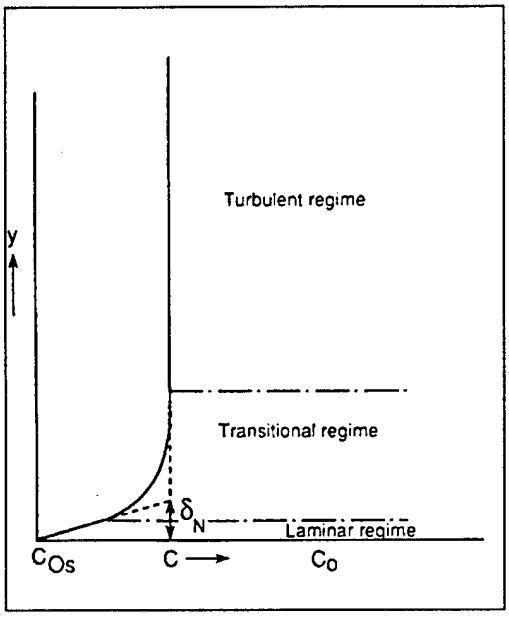

C_{Os} = concentration of species O at the electrode surface
C_o = bulk concentration of species O
δ_N = thickness of diffusion layer.

(Source: Goodridge and Scott 1995. Used with permission).

Figure 10. Concentration profile for a fully developed turbulent flow.

Disregarding for a moment any migration phenomena, a rigorous calculation of the mass flux would have to find quantitative expressions for mass transport in the turbulent bulk. Unfortunately, the treatment of turbulent flow of liquids is much more complex than that for laminar flow. The following simple model, called the film model or film theory, is commonly used for characterizing turbulent flow.

The first assumption is that mass transport due to eddy diffusion in the turbulent bulk is so fast when compared to molecular diffusion that the latter can be ignored and a uniform concentration of the bulk can be assumed. The second assumption is that all resistance to the mass transfer process can be expressed in terms of molecular diffusion in the laminar sublayer. Thirdly, this resistance can be expressed quantitatively by assuming a completely linear concentration gradient, including in this way the effect of the buffer layer. The point where the linear concentration gradient meets the horizontal bulk concentration defines the thickness of a layer called the diffusion boundary layer (δ_N). The flux, N_D, can be calculated by deriving an expression for the molecular diffusion of O through a stagnant layer of thickness δ_N. Using Fick's diffusion equation:

$$\partial c/\partial t = D\, \partial^2 c/\partial y^2 \qquad \text{(Eq 12)}$$

where c is the concentration at time t and coordinate y of species O, and D is its diffusivity.

For a steady state condition, Equation 12 reduces to

$$d^2c/dy^2 = 0 \qquad \text{(Eq 13)}$$

The boundary conditions depicted in Figure 10 are:

$$c = c_{Os} \qquad y = 0 \qquad \text{(Eq 14)}$$

$$c = c_O \qquad y = \delta_N \qquad \text{(Eq 15)}$$

The diffusional flux of O to the electrode surface N_D is given by Fick's law:

$$N_D = -D(dc/dy)_{y=0} \qquad \text{(Eq 16)}$$

Solving the above results in:

$$N_D = D\,(c_O - c_{Os})/\delta_N \qquad \text{(Eq 17)}$$

$$N_D = k_L (c_O - c_{Os})$$

where $k_L = D/\delta_N$ and is also known as the mass transfer coefficient.

There are different methods of evaluating the mass transfer coefficient k_L. It can be found either by calculations or by experimental methods. Some of the numerical methods for estimating k_L are listed below.

For rectangular flow channels (Figure 11):

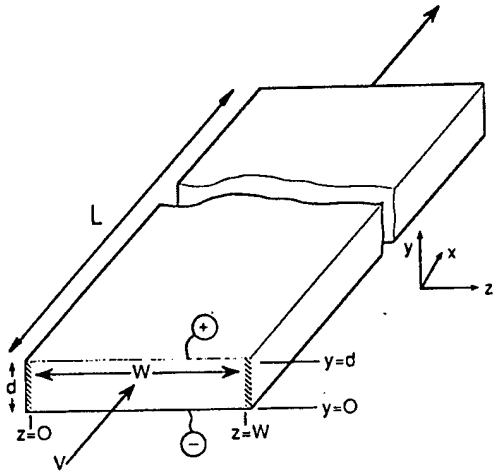

(Source: Goodridge and Scott 1995. Used with permission).

Figure 11. Rectangular flow channel.

For laminar flows:

$$Sh = 2.54[(Re)(Sc)(d_e/L)]^{0.3} \quad \text{(Eq 18)}$$

where Sh (Sherwood number) = $k_L d_e/D$; Sc (Schmidt number) = ν/D; Re (Reynolds number) = ud_e/ν; and $d_e = 2d$

Developing laminar flow:

$$Sh'_x = 0.96\, Re_x^{0.5}\, Sc^{1/3}\, (d_e/L)^{-0.05} \quad \text{(Eq 19)}$$

where $Sh'_x = k_{L,x}\, x/D$ and $Re_x = ux/\nu$. For design purposes, however, it is better to use a form of Equation 19 to ensure a conservative estimate of k_L.

For turbulent flow:

$$Sh = 0.023Re^{0.8} Sc^{1/3} \quad \text{(Eq 20)}$$

The Annulus (Figure 12):

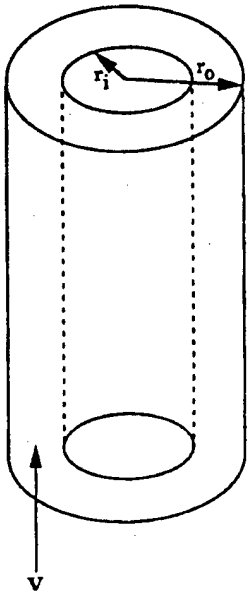

r_i = radius of the inner cylinder;
r_o = radius of the outer cylinder.

(Source: Goodridge and Scott 1995. Used with permission).

Figure 12. Annulus between two concentric cylinders with axial flow.

For laminar flow:

$$Sh = 1.614[\Phi ReSc(d_e/L)]^{1/3} \quad \text{(Eq 21)}$$

where $d_e = 2(r_o - r_i)$, and Φ is a geometric parameter defined as:

$$\Phi = [(\frac{1-r}{r}) \frac{(0.5 - \frac{r^2}{1-r^2}\ln[1/r])}{(\frac{1+r^2}{1+r^2}\ln[1/r] - 1)}]$$

where $r = r_i/r_o$.

For turbulent flow, Equations 19 and 20 are used.

For rotating cylinder electrodes (Figure 13):

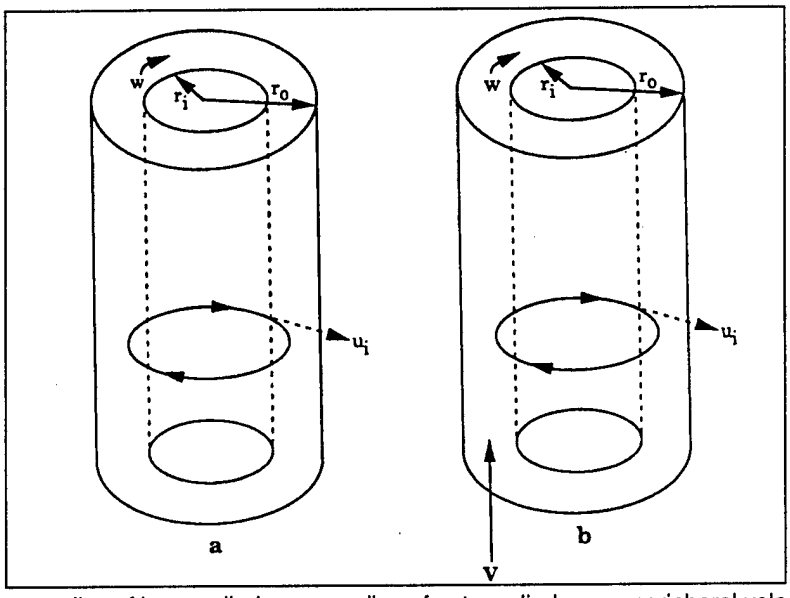

r_i = radius of inner cylinder; r_o = radius of outer cylinder; u_i = peripheral velocity; w = angular velocity.

(Source: Goodridge and Scott 1995. Used with permission).

Figure 13. Rotating cylinder: (a) no axial flow and (b) with axial flow.

An important application of the concentric cylinder arrangement is when one of the cylinders rotates. In the more popular system, the inner cylinder is rotating while the outer one is stationary. This system is preferred to the situation where the outer cylinder is rotating, for two reasons:

1. Lower rotational speeds are required to produce turbulence and hence good mass transfer characteristics.
2. The design is mechanically less complicated.

The hydrodynamics of the flow between the two cylinders can be characterized by a dimensionless quantity Ta, the Taylor number, and is defined as:

$$Ta = [\frac{u_i(r_o - r)_i}{\upsilon}][\frac{r_o - r_i}{r_i}]^{1/2} = \mathrm{Re}_w[\frac{r_o - r_i}{r_i}]$$

where u_i is the peripheral velocity of the rotating cylinder. Based on the Taylor number, three flow regimes can be distinguished:

1. At low flow rates, a simple laminar (or Couette) flow prevails in which the velocity of the fluid is tangential. This region is characterized by Ta < 41.3,

which offers little enhancement of mass transport and is of no consequence to reactor design.

2. At higher flow rates, the simple tangential flow becomes unstable and a cellular motion is superimposed upon the tangential flow. The "Taylor vortices" carry material from one cylinder to the other, thereby increasing mass transfer rates. However, because of the cellular or vortex nature of the flow, the mass transfer characteristics are not uniform. The region is characterized by $41.3 < Ta < 400$.

3. At high flow rates ($Ta > 400$), the flow becomes turbulent, characterized by random and rapid fluctuations of velocity. Theoretical analyses of this regime agree in general with experimentally obtained correlations, and in particular with the extensive data of Eisenberg, Tobias, and Wilke (1954) for a range of Re_w of 100-160,000. Their correlation for an annular space of > 8mm is:

$$St_w = k_L/u_i = 0.0791\ Re^{-0.3}\ Sc^{-0.644} \qquad \text{(Eq 24)}$$

where Stanton number, $St_w = Sh_w/Re_wSc$.

For obtaining the value of k_L for kinetic calculations, the limiting current technique is used. As discussed earlier, the limiting current density is the current density at which the rate limiting step is the rate at which reactant molecules reach the electrode and is given by:

$$i_{lim} = nFk_Lc_o \qquad \text{(Eq 25)}$$

where n is the number of electrons involved in the reaction, F is the Faraday's Constant, and c_o is the concentration of the molecule to be electrochemically reduced.

Reaction Modeling

An electrode process may proceed through all or some of the following steps:

1. The electroactive species is transferred to the electrode surface from the bulk solution.

2. The electroactive species is adsorbed on the electrode surface.

3. Electrons are transferred between the electrode and the reacting species.

4. The reacted species suffers desorption and chemical reaction, in either order, then is transported back into the bulk solution.

If r_- and r_+ are the chemical forward and backward reactions, multiplying by nF converts these reaction rates to current densities i_- and i_+ respectively. According to the Butler-Volmer equation, in the absence of a concentration gradient:

$$i_c = i_- - i_+ = i_o \{ \exp[-\alpha\eta nF/RT] - \exp[(1-\alpha)\eta nF/RT]\} \quad \text{(Eq 26)}$$

where i_c is the net amount of reaction occurring and α is the transfer coefficient.

If the charge transfer step is rate-controlling, conditions at the electrode interface will be far from equilibrium except at very low current densities (i.e., $i_- >> i_+$) and therefore $i_c \approx i_-$. This "Tafel Approximation" gives:

$$i_c = i_o \exp[-\alpha\eta nF/RT] \quad \text{(Eq 27)}$$

It follows that, for conditions far removed from equilibrium, a plot of cathodic overpotential against $\ln[i_c]$ (Figure 14) will give a straight line of slope $(RT/\alpha nF)$ and an intercept of $\ln[i_o]$ on the logarithmic coordinate. This kind of plot is called a Tafel curve and the slope is referred to as the Tafel slope.

For anodic reactions, the slope is $[RT/(1-\alpha)nF]$.

For very small values of η (indicating that the electrode is operating near equilibrium), Equation 27 can be linearized to:

$$(i_c/i_o) = (-\eta nF/RT) \quad \text{(Eq 28)}$$

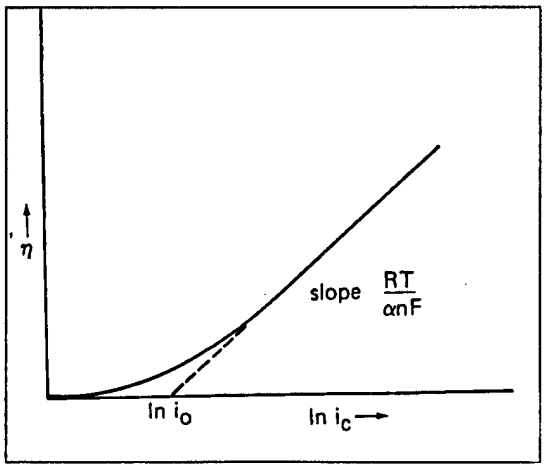

(Source: Goodridge and Scott 1995. Used with permission).

Figure 14. A typical Tafel Plot.

The greater the value of i_o, the greater the net current that can be supported by the electrode under reversible conditions. The corollary is that electrode reactions characterized by high exchange currents are less likely to show charge transfer control.

Look at the simple reaction:

$$A + ne^- \rightarrow B \qquad \text{(Eq 29)}$$

As shown in Figure 15, for the reaction to occur, A has to be transported to the electrode, charge transfer (possibly via intermediates) occurs resulting in product B, which is then transported back into the bulk of the electrolyte.

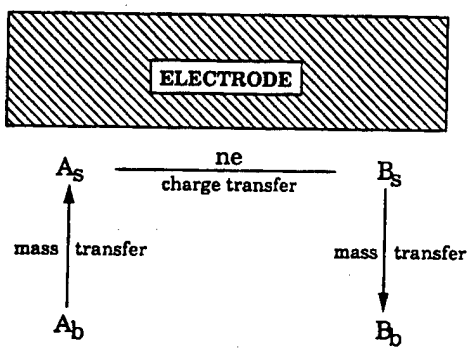

(Source: Goodridge and Scott 1995. Used with permission).

Figure 15. Simple reaction mechanism.

The rate of diffusional transport of A to the electrode is given by:

$$dQ_A/dt = k_L S(c_A - c_{As}) \qquad \text{(Eq 30)}$$

where Q_A is the number of kmols of A transported to the electrode surface, t is the time, k_L is the mass transfer coefficient, S is the electrode surface area, and c_A and c_{As} are the concentration of A in the bulk and near the surface.

The equation that provides r_A, the rate of reaction of A at the electrode surface, has the form:

$$r_A = Sf(c'_{As}, E', ..) \qquad \text{(Eq 31)}$$

where the functional relationship f describes the reaction kinetics in terms of c'_{As}, (the surface concentration of A), E' (the electrode potential), and any other parameters required to define the kinetics. In practice, c_{As} and c'_{As} are equated or an adsorption isotherm is used.

At steady state:

$$r_A = dQ_A/dt \quad \text{(Eq 32)}$$

Assume for simplicity's sake that $c_{As} = c'_{As}$. Converting Equations 31 and 32 to current densities yields the following:

$$i = nFk_L(c_A - c_{As}) \quad \text{(Eq 33)}$$

$$i = nFf(c_{As}, E',...) \quad \text{(Eq 34)}$$

Equating Equations 33 and 34 enables the elimination of surface concentrations and results in a single expression for the current density in terms of the aforementioned parameters.

Assuming a primary reaction A → B, which is governed by a simple "Tafel-type" expression, one can develop a typical expression for a reaction model. Equation 34 becomes:

$$i_A = nFk'_A c_{As} \exp(-b_A E') = k_A c_{As} \exp(-b_A E') \quad \text{(Eq 35)}$$

where i_A is the partial current density for the formation of product B and b_A is the slope of the polarization curve obtained by plotting $\ln[i_A]$ against E'. Also, k'_A and k_A are reaction rate constants, where $k_A = nFk'_A$. The reason Equation 35 is used in reaction modeling is that many industrial systems are not reversible and hence the use of i_o, the exchange current density, and η, the overpotential, is not possible.

Eliminating c_{As} from Equations 33 and 35:

$$i_A = \frac{c_A}{\frac{1}{nFk_L} + \frac{1}{k_A \exp[-b_A E']}}$$

Primary reaction may be accompanied by an independent secondary reaction, often associated with the decomposition of the solvent or the discharge of a secondary ion. The secondary reaction for aqueous cathodic process is, typically, hydrogen evolution. A simple Tafel relationship is assigned to the secondary reaction, because mass transfer plays only a minor role in the discharge process; the concentration term is omitted on the assumption that the solvent

composition will change insignificantly during electrolysis. The partial current density for hydrogen evolution, i_H, is:

$$i_H = k_H \exp [-b_H E'] \quad \text{(Eq 37)}$$

To obtain a reaction model, one needs the numerical values for the kinetic constants: k_A, b_A, k_H, and b_H as well as a value for k_L.

3 Electrochemical Degradation of 2,4,6-TNT, 2,4-DNT, and RDX

Important Parameters

The roles of stirring rate, current, surface area, and pH were investigated for the three nitro-aromatics separately and in combination with each other (to simulate the munitions wastewaters more closely and to find out if there is any inhibitory effect on degradation rates due to the combination). Product identity is important for any degradation process development, so the identification of the products was an additional focus of this study. Finally, it was important to identify the mass transfer limitations occurring in the system and to reduce them through more efficient hydrodynamics, keeping in mind the final reactor design.

Experimental Setup

Experiments were carried out in a 2.5-L glass reactor. A Nafion membrane #117 (Solution Technology/C.G.Processing, Rockland, DE) was used to separate the anode and the cathode, to allow the transfer of ions only, and to prevent the transfer of any of the organic compounds being degraded or being formed. A Universal Digital Controller (UDC) 300 (Honeywell, York, PA) was used as a constant current source. A Thermix® Stirrer Model 120S (Fisher Scientific, Pittsburgh, PA) was used for all experiments along with a 2-in. Teflon-coated stir bar. Two types of cathode were used: a 150-mm long, high density fine grain graphite annular cylinder with an inner diameter of 63 mm and outer diameter of 83 mm from Graphite Sales, Inc. (Chagrin Falls, OH), and a glassy carbon (Sigradur® G) rod with a diameter of 7 mm and a height of 150 mm from SGL Carbon Corporation (St. Marys, PA). The properties of the carbon electrodes are shown in Table 1. A 6-in. long 18G platinum wire (Fisher Scientific) was used as the anode.

TNT was obtained containing 30 weight percent water and was used as such by making appropriate adjustments while weighing the TNT to be added into the reactor. DNT was obtained at 97 percent purity and was used as received. RDX was obtained at 99 percent purity and was used as received. Sodium phosphate was used as the buffer to maintain the desired pH. Anhydrous sodium sulfate

was added to the reactor to maintain a constant ionic strength. All experiments were carried out in a 2-L solution of the reaction mixture. For all experiments, 18 MW-cm resistivity water was used (distilled and deionized). Each nitroaromatic was added to the reactor yielding an initial concentration of 50 ppm. The initial sodium sulfate concentration was 36 g/L and 0.02 M phosphate buffer adjusted to desired pH was used for all experiments. The pH was monitored throughout the experiments and a few drops of a 1 M sulfuric acid solution were added regularly to maintain the solution at the desired pH. An Oakton® WD-35615-Series pH/mV/temperature meter was used as the pH probe. Figure 16 is a diagram of the reactor. The reactor conditions are summarized in Table 2.

Table 1. Physical properties of the glassy carbon cathode.

Property	Graphite Cylinder	Sigradur® G
Maximum Grain Size	0.84 mm	-
Apparent Density	1.68 - 1.71 g/cm^3	1.42 g/cm^3
Total Porosity	21 %	0 %
Electrical Resistivity	6.5-7.5 x 10^6 µohm-cm	4.4 x 10^3 µohm-cm
Flexural Strength	170-240 kg/cm^2	2.6 x 10^5 kg/cm^2
Compressive Strength	300-400 kg/cm^2	4.8 x 10^5 kg/cm^2
Modules of Elasticity	1100-1250 kg/mm^2	35000 kg/mm^2
Ash	0.20 %	0 %

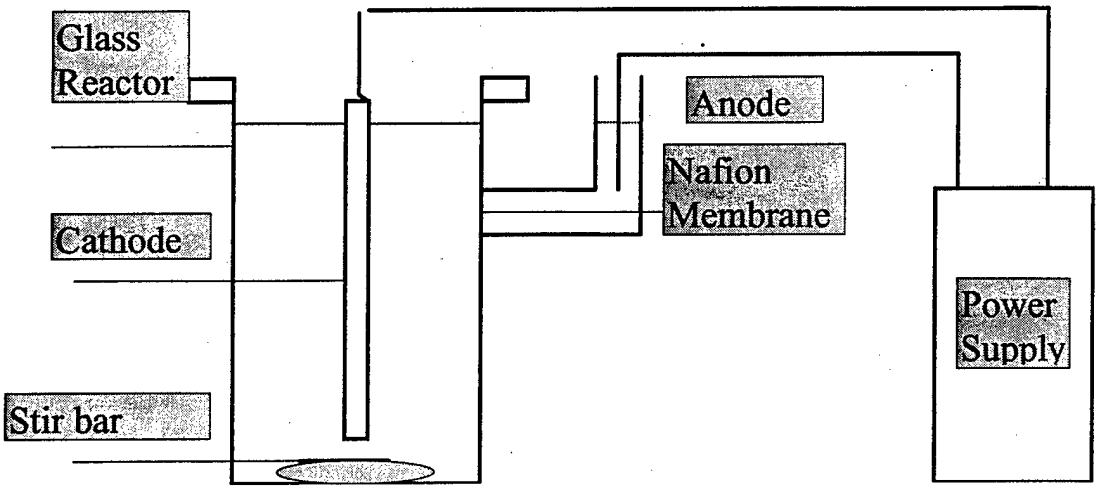

Figure 16. Experimental setup for the batch experiments.

Table 2. A summary of experimental conditions.

Serial No.	Parameters	Values
1	Reactor Volume	2000 ml
2	Salt Concentration	36 g/l
3	Initial Nitro-aromatic Concentration	50 ppm
4	pH	8
5	Applied Current	23mA - 65mA
6	Stir rate	540 -2500 rpm
7	Electrodes	Graphite Glassy Carbon (Sigradur® G)
8	Surface area	67.5 cm^2 (Glassy Carbon).
9	Porosity	21% (Graphite) 0% (Glassy Carbon)
10	Dissolved Oxygen	0.2 mg/L (Deoxygenated) 8.4 mg/L (Open System)

Analytical Techniques

The length of time for one experiment was always less than 12 hr. Six to eight samples were taken at regular intervals in each experiment. When the samples were taken, researchers also monitored pH, voltage, dissolved oxygen (DO), oxidation-reduction potential (ORP) and conductivity. TNT and DNT were analyzed by gas chromatography (GC). GC samples were withdrawn from the reactor with a 2.5 mL pipette. The samples were then extracted into 0.5 mL of dichloromethane with vigorous shaking for 2 minutes. An internal standard of quinoline (25 ppm) was used for analysis precision. The GC instrument used in the analysis is an HP 5890 Series II with an FID detector, 30 m x 0.32 mm i.d. fused silica capillary column and 0.25-mm film thickness (J & W Scientific, Folsom, CA, DB-1), and a carrier gas of nitrogen (80 psi).

RDX was analyzed by a Shimadzu UV-1201 spectrophotometer. 10ml samples of the solution in the cathodic compartment were withdrawn at the pre-determined intervals and measured by UV absorption using the spectrophotometer at a wavelength of 240 nm. Minimal UV absorption by other components of the solution at this wavelength has been ascertained.

The pseudo-first-order rate constants were obtained by plotting the natural log of the nitro-aromatic concentration in ppm versus time in minutes. Only the kinetic data with an R^2 value more than 0.95 are reported.

Samples for gas chromatography-mass spectrometry (GC-MS) for product identification were withdrawn from the reactor once or twice: a larger 50 mL sample was taken and extracted into benzene, dichloromethane, or diethyl ether. At the end of each experiment, 250 mL was saved for further extraction to identify the final products. All samples were kept at 4 °C until analyzed.

The GC analysis allowed the monitoring of the degradation of DNT and the formation of intermediates and products. The GC-MS analysis allowed the identification of stable intermediates and final products. The GC-MS instrument is an HP 5890 GC and MS 5970, a selective mass ion detector, 30 m x 0.25 mm i.d. fused silica capillary column and 0.25 mm film thickness (J & W Scientific, DB-5), and a carrier gas of He (50 psi).

The intermediates and end products of degradation of TNT were found to be thermally unstable. Therefore, no distinct peaks are observed in either the GC or the GC-MS of these products. To identify and quantify these intermediates and products, HPLC was used with the following specifications: an HP 1050 system using a C-18 column, with a Quaternary pump and a UV Diode Array Detector (DAD). The EPA 8330 method was used. The HPLC-18 column was eluted with 5.4:4.6 acetonitrile/water at a flow rate of 1.5 mL/min. An internal library was constructed by analyzing pure compounds and then the compounds in the reactor solution were identified by matching the UV absorbance spectra and retention time. The pure intermediates and products were purchased, if available commercially, or were otherwise synthesized.

The ORP was measured using a double-junction ORP electrode (Cole Parmer Instrument Co., Vernon Hills, IL) with a platinum band. The electrode was tested before use with two different buffers (pH 4.0 and 7.0) saturated with quinhydrone. This test showed the calibration to be correct and that the probe was functioning properly according to the range of ORP values given by the manufacturer. The ORP electrode was rinsed with deionized water and the ORP was measured directly in the reactor.

Synthesis of Selected Degradation Products

Some of the expected products were commercially unavailable, so a literature search was conducted to assess the feasibility of synthesizing them in the laboratory. The following experimental methods were used for the synthesis of selected by-products.

Synthesis of 4,4'-dinitro-2,2'-azoxytoluene (2,2' Azoxy Dimer)

- 1.52 g (10 mmol) of 2-amino-4-nitrotoluene was added to 75 mL of dichloromethane.
- g (20 mmol) of m-chloroperoxybenzoic acid was added to the above solution and allowed to stand overnight.
- The precipitate of chlorobenzoic acid was removed by filtration and the filtrate extracted with 5 percent aqueous sodium bicarbonate solution.
- The dichloromethane was allowed to evaporate and the resulting precipitate was recrystallized with 95 percent ethanol.
- A slightly yellow solid of the dimer was collected.

The above procedure is repeated with 4-amino-2-nitrotoluene as the starting compound to produce the other possible isomer (McCormick, Cornell, and Kaplan 1978).

Synthesis of Caroís Acid

- 145 g (0.64 moles) of ammonium persulfate was added to 54 mL of cold, concentrated H_2SO_4.
- The mixture was allowed to stand for about 1 hr and poured into 355 g of crushed ice.

Synthesis of 2-nitro,4-nitroso Toluene

- A cold suspension of 3.5 g (0.23 mole) of 2-nitro,4-amino toluene in 6 mL of sulfuric acid and 1 mL of water is mixed in an ice bath for 1 hr.
- Caroís acid is added to the above and stirred for 17 hr. The yellow precipitate was recrystallized with acetone.

Synthesis of 2,2',6,6'-tetranitro,4,4'-azoxytoluene (4,4' Azoxy Dimer)

- A vigorously stirred solution of 0.062 mole of 2,4,6-trinitrotoluene was prepared in 75 mL of acetic acid and 10 mL of acetic anhydride.

- The temperature was maintained throughout between 30 °C and 35 °C by adjusting the addition rate of zinc dust and providing the heating or cooling as needed.

- 12.0 gm of zinc dust is added over a 1.5-hr period.

- The pasty reaction mixture is then diluted with 1 L of ice water and solid is separated by filtration.

- The solid product is then treated for 15 min with 300 mL of a 10 percent aqueous sodium carbonate solution at 40 °C.

- The product is filtered and pressed dry. The solid is then dissolved in warm ethanol.

A solid crystallizes out on drying (Sandler and Karo 1971). However, when the solid was analyzed on GC-MS, no prominent peak was observed.

Other chemicals (4-amino-2,6-dinitrotoluene; 2-amino,4,6-dinitrotoluene; 2,2', 6,6'-trinitro,4,4'-azoxytoluene, and 4,4',6,6'-trinitro,2,2'-azoxytoluene) were obtained commercially.

Degradation Behavior as a Function of Various Parameters

Effect of Dissolved Oxygen

Deoxygenated experiments were carried out to see the effect of dissolved oxygen on the product distribution, especially since the main end-product of electrocatalytic hydrogenation of DNT (i.e., DAT) is unstable in the presence of oxygen. These experiments were carried out by keeping the reactor closed to the atmosphere. A lid with a spring lock and ports for removing samples and inserting the electrodes was used to close the reactor and make it airtight. Figure 17 shows the experimental setup.

The reactor was then purged with nitrogen with the help of a diffuser until the dissolved oxygen in the reactor decreased to 0.2 mg/L. The dissolved oxygen was measured with a Corning Checkmate 90 dissolved oxygen meter (Corning, NY). Before use, the dissolved oxygen probe was calibrated at one calibration point. The setting should be 100 percent saturation, which can be achieved by using air calibration. The 100 percent calibration was set by holding the probe 1 cm above

a beaker of water. Sampling was carried out using a syringe, which was pierced through a septum in the lid.

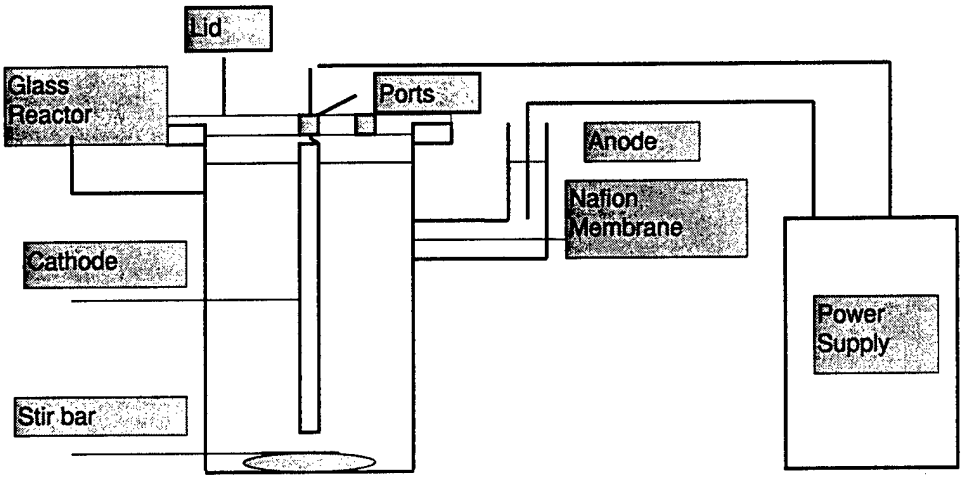

Figure 17. Experimental setup for deoxygenated experiments.

Effect of Surface Area of the Cathode

These experiments were carried out using the glassy carbon cathode only, because the surface area can be determined accurately only for the glassy carbon, which has a zero porosity. The surface area was varied by changing the height of the cathode immersed inside the reactor solution. The change in reaction rate for five different surface areas was determined. The degradation rates increased with the increase in the surface area.

Effect of pH of the Cathodic Solution

The pH was expected to be a sensitive parameter in the overall degradation mechanism since the availability of protons (hence the concentration of the reactive hydrogen radicals) is determined by the pH of the solution. The pH was varied by adding to the buffered solution — either sulfuric acid or sodium hydroxide as required. Experiments used pH settings between 6.0 and 9.0. Degradation rates were found to increase, by both lowering and increasing the pH from the original value of 8.0.

Effect of the Electrode

Two different electrodes were used to study which was more effective in the electrochemical degradation of DNT. A glassy carbon electrode was evaluated due to its smooth nonporous surface, which would reduce the possibility that hydrogen might build up (and block the access of the water to the electrode). As discussed

earlier, the glassy carbon electrode has a porosity of 0 percent; hence the determination of the effective surface area becomes much easier.

Product Studies and Mass Balance

Electrochemical Reduction of DNT

It is important to identify the stable intermediates and products to determine the possible reaction pathways. Moreover, it has to be determined whether the products are environmentally more harmful than the starting compound DNT.

For product identification, the sample from the reactor underwent GC-MS analysis. From the MS diagram of each compound, one can find the molecular weight of the compound as well as its main molecular fragments. By comparing the molecular weight and the fragmentation pattern of found products with those of compounds in the reported literature on DNT degradation, the compound can be identified. Analyzing this compound by GC-MS and comparing the retention times of the various isomers with those of the unknown products reveals the identity of the correct isomer.

According to available literature, the end-product of 2,4-dinitrotoluene hydrogenation is 2,4-diaminotoluene, while the possible intermediates are the azoxy dimer, nitroso- nitrotoluene and hydroxylamino-nitrotoluene (Figure 1; McCormick, Cornell, and Kaplan 1978; Neri et al. 1995). DAT has been identified as one of the main products. DAT 97 percent purity was used as purchased. The synthesis of the azoxy dimer (McCormick, Cornell, and Kaplan 1978) and the nitroso-nitrotoluene (Sandler and Karo 1971) was presented previously.

Effect of Treatment Parameters

The pseudo-first-order rate constants for DNT were examined to determine the influence of parameters such as cathode material, surface area, stir rate, current, and oxygen. Only experimental data with an R^2 value of greater than 0.95 for the linear fit for ln[DNT Conc] vs time curve were reported. Table 3 shows the rate constants for experiments performed with the graphite cylinder. Table 4 shows the rate constants for experiments performed with the glassy carbon. Table 5 shows the effect of surface area on the reaction rate constant.

Table 3. Experimental data for a graphite cylinder cathode.

Current (mA)	Stir rate (rpm)	Dissolved Oxygen	Rate Constant (min^{-1})
65	630	Open System	0.0076
65	2040	"	0.01
53	630	"	0.0106
53	2040	"	0.0154
45	630	"	0.007
45	2040	"	0.0088
23	630	"	0.0045
23	2040	"	0.0009
65	630	Deoxygenated	0.0105
65	2040	"	0.0168
53	630	"	0.0145
53	2040	"	0.0146
45	630	"	0.0125
45	2040	"	0.0139
23	630	"	0.005
23	2040	"	0.0059
Note: Surface area = 722 cm^2.			

Table 4. Experimental data for a glassy carbon cathode.

Current (mA)	Stir rate (rpm)	Dissolved Oxygen	Rate Constant (min^{-1})
65	630	Open System	0.0053
65	2040	"	0.0068
45	630	"	0.0048
45	2040	"	0.0062
23	630	"	0.0038
23	2040	"	0.0044
65	630	Deoxygenated	0.0052
65	2040	"	0.005
45	630	"	0.004
45	2040	"	0.0049
23	630	"	0.0042
23	2040	"	0.0047
Note: Surface area = 57.9 cm^2.			

Table 5. Experimental data for the effect of surface area on DNT degradation.

Surface Area (cm^2)	Rate Constant (min^{-1})
67.5	0.008
57.9	0.0068
44.75	0.0049
31.35	0.0035
Note: Glassy carbon cathode, stir rate = 2040 rpm, current = 65mA.	

These results are graphically summarized in Figures 18 through 22.

Effect of Current

As shown in Figures 18 through 21, the reaction rate increases with an increase in current. This increase is due to the current density being a direct measure of the reaction rate. The rise in reaction rate, however, is not linear and seems to level off or drop in some cases. Charge transfer is the rate limiting step until the current density reaches the limiting current density (i_{lim}). The limiting current density for the glassy carbon electrode is 10 mA/m2, which corresponds to a current of 57.9 mA. This limiting current, however, is the partial current density for DNT alone and not the total current density, which is why there is still an increase in the reaction rate at 65 mA. Therefore, as the current density approaches the limiting current density, the mass transfer rate becomes more and more dominant and beyond i_{lim} there is no major increase in reaction rate with an increase in current density. This explains the leveling behavior of the reaction rate with an increase in current. The fact that mass transfer becomes more important with an increase in current becomes evident in Figure 18, where the difference between reaction rates at different stir rates become more pronounced at higher currents.

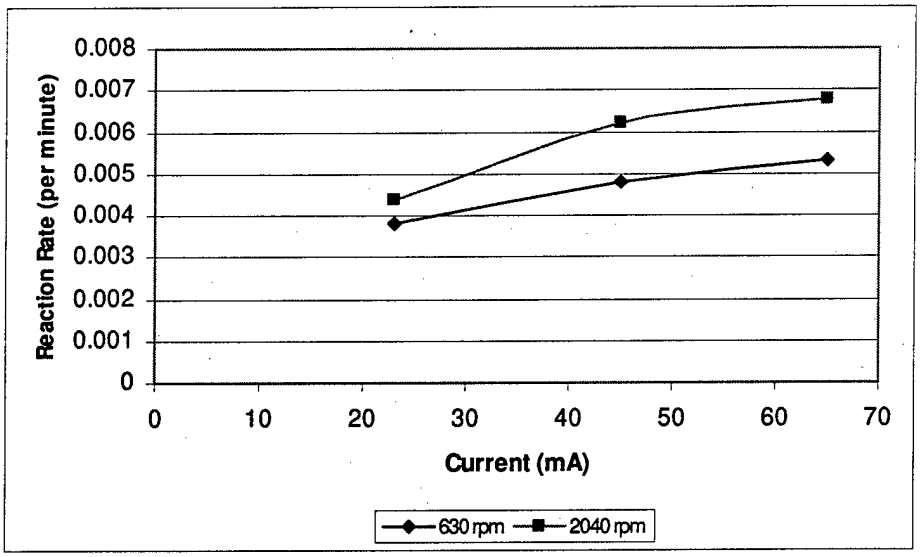

Figure 18. Plot of reaction rate vs current for a glassy carbon electrode (open system) for two different stir rates.

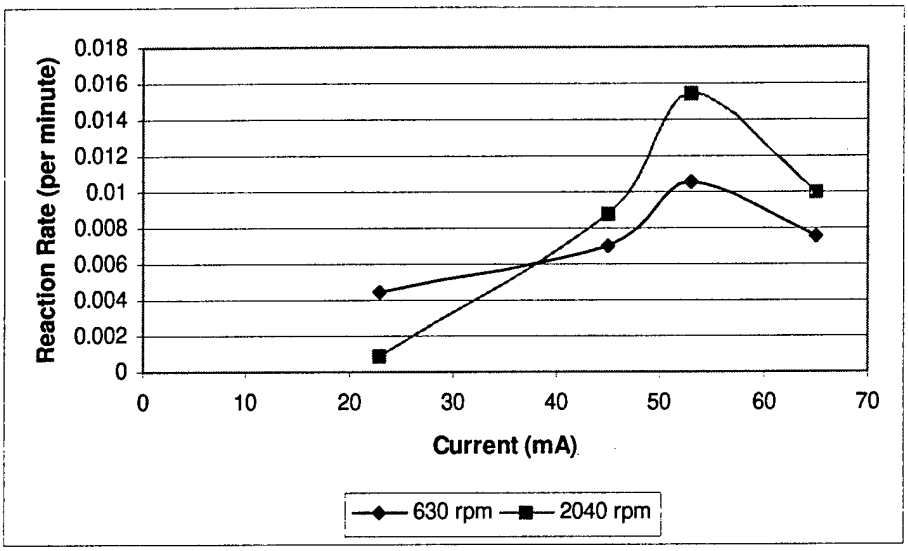

Figure 19. Plot of reaction rate vs current for a graphite cylinder electrode (open system) for two different stir rates.

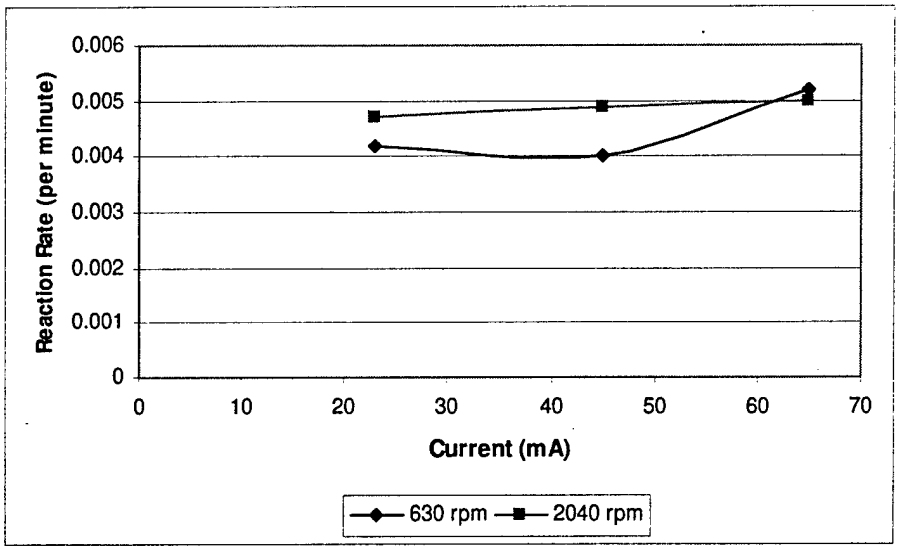

Figure 20. Plot of reaction rate vs current for a glassy carbon electrode (deoxygenated system) for two different stir rates.

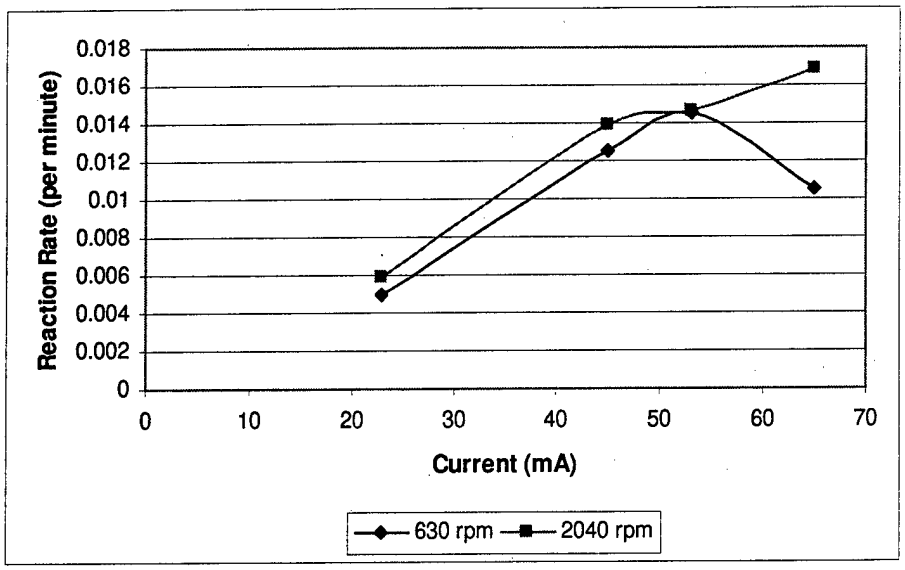

Figure 21. Plot of reaction rate vs current for a graphite cylinder electrode (deoxygenated system) for two different stir rates.

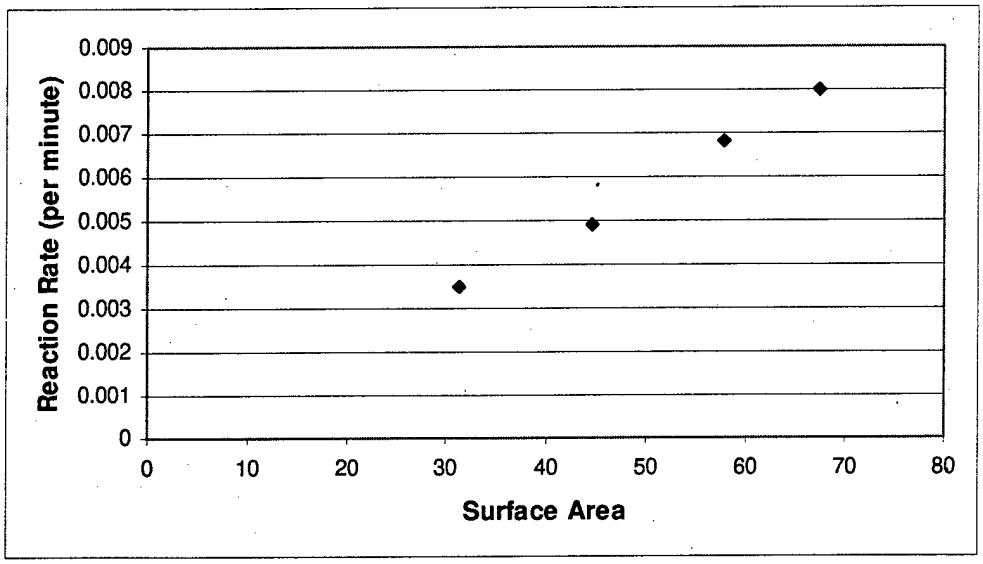

Figure 22. Dependence of reaction rate on the surface area of the electrode (glassy carbon electrode).

In the case of the graphite cylinder electrode, there is a dramatic reduction in reaction rate at a current of 65 mA. This reduction could be because of the deposition of particulate reaction products inside the pores, which means a reduction in the effective surface area. This conclusion can be supported by the fact that, except for the 65 mA current setting, the mass balance relating DNT concentration and the various product concentrations are complete for all other current settings and also for the glassy carbon electrode.

Effect of Stir Rate

Experiments were carried out at different stir rates to see the effect of mass transfer on the reaction rate. From the experimental results for both electrodes, it was seen that the reaction rate increased with an increase in stir rate. This increase was due to the fact that, with an increase in stir rate, the velocity component perpendicular to the surface of the electrode increased. Since the experiments were carried out close to the limiting current density of the glassy carbon electrode, an increase in velocity increased the mass transfer coefficient thereby increasing the reaction rate. A higher stir rate also decreases the chance of any of the inert products such as the azoxy dimer from being adsorbed onto the electrode surface and lowering the surface area available for electrochemical reduction of DNT.

Effect of Dissolved Oxygen

Dissolved oxygen experiments were carried out to see the effect of oxygen on the product distribution. Tables 6 and 7 show that, in the open system experiments the main products formed were the dimers, whereas in the deoxygenated experiments the main product formed was DAT. This difference in product can be explained by the fact that a two-stage reaction mechanism is operative and an intermediate is being formed, which either gets reduced to DAT or gets oxidized to the azoxy dimer. In the absence of oxygen, the only pathway is that of total reduction to DAT. Further discussion on the effects of the presence and absence of oxygen can be found in the following sections.

Effect of Surface Area

Figure 22 shows that, with an increase in surface area, there is an increase in the reaction rate. This result is due to the fact that an increase in surface area makes the charge transfer more effective; hence the reaction rates are enhanced.

Table 6. Summary of residence times of various products and intermediates.

Compound Name*	Retention Time in GC-MS (min)	Retention Time in GC (min)
DNT	17.027	5.759
DAT	12.7	4.642
Dimer-1	31.91	11.09
Dimer-2	32.38	11.628
AN-1	18.22	6.144
AN-2	17.32	5.715
Nitroso-1	14.7	5.23
* DAT = 2,4-diaminotoluene; DNT = 2,4-dinitrotoluene; D-1 = 4,4'-dinitrotoluene,2,2'-azoxytoluene; D-2 = 2,2'-dinitrotoluene,4,4'-azoxytoluene; Nitroso-1 = 2-nitroso,4-nitrotoluene; AN-1 = 2-amino,4-nitrotoluene; AN-2 = 4-amino,2-nitrotoluene		

Table 7. Product distribution.

Cathode: Graphite Cylinder (open system)			
Current (mA)	**Compounds**	**Solid Phase (%Molar Conversion of DNT to:)**	**Aqueous Phase (%Molar Conversion of DNT to:)**
65	DAT	-	28.5
	D-1	2.23	4.21
	D-2	43.9	-
	Total	46.13	32.71

Total Mass Balance (%Molar Conversion of DNT to Identified Products) = 78.84%

45	DAT	-	23
	D-2	87.8	-
	Total	87.8	23

Total Mass Balance (%Molar Conversion of DNT to Identified Products) = 110%

Cathode: Glassy Carbon (open system)

Current (mA)	**Compounds**	**Solid Phase (%Molar Conversion of DNT to:)**	**Aqueous Phase (%Molar Conversion of DNT to:)**
65	DAT	-	37.7
	D-2	58.7	-
	Total	58.7	37.7

Total Mass Balance (%Molar Conversion of DNT to Identified Products) = 96.4%

45	DAT	-	24.2
	Nitroso-1	-	10.7
	D-1	7.7	-
	D-2	65.96	-
	Total	73.66	34.9

Total Mass Balance (%Molar Conversion of DNT to Identified Products) = 108.6%

Current (mA)	**Compounds**	**Solid Phase (%Molar Conversion of DNT to:)**	**Aqueous Phase (%Molar Conversion of DNT to:)**
23	DAT	-	22.7
	Nitroso-1	-	6.6
	AN-1	-	7.13
	D-1	7.89	-
	D-2	42.9	27.6
	Total	50.8	64

Total Mass Balance (%Molar Conversion of DNT to Identified Products) = 114.8%

Cathode: Glassy Carbon (Deoxygenated system)

Current (mA)	**Stir rate (rpm)**	**DAT Conc (ppm)**	**%Molar conversion of DNT to DAT**
23	630	25.7	76.7
23	2040	32.0	96.0
45	630	28.2	98.0
45	2040	27.7	95.0
65	630	20.9	70.0
65	2040	24.4	78.9

Effect of Electrode Selection

The experimental results show that, even though the surface area of the glassy carbon electrode is much smaller than that of a graphite cylinder electrode, the reaction rates are comparable. This implies that the reaction rate per unit surface area of the electrode is much greater for a glassy carbon electrode than for a graphite cylinder electrode. Comparing the physical properties of these two electrodes in Table 1 shows the electrical resistivity of the graphite electrode is approximately three orders of magnitude greater than that of the glassy carbon electrode. A lower resistivity implies a higher conductivity for the glassy carbon electrode, which in turn enhances the charge transfer. This results in better degradation of DNT by the glassy carbon electrode.

Product Identification and Mass Balance

All the possible intermediates were either purchased or synthesized based on their availability as discussed previously. Table 6 summarizes the retention times of the various possible intermediates in both the GC-MS and the GC.

The compounds that have been identified as having been formed as intermediates and products are 2,4-diaminotoluene, 4,4'dinitro,2,2'-azoxytoluene, 2,2'-dinitro,4, 4'-axozytoluene, 2-amino,4-nitrotoluene, and 4-amino,2-nitrotoluene. The major product was 2,2'-dinitro,4,4'-azoxytoluene (Dimer-2) in the open system and 2,4-diaminotoluene in the deoxygenated system.

Based on the identified compounds and the various mechanisms reported in literature, the most probable reaction pathway in the electrochemical degradation of DNT is that reported by McCormick, Cornell, and Kaplan (1978; Figure 1), with the pathway leading to the formation of Dimer-2 being the most dominant. The hydroxyl-amine could not be synthesized because of its instability in the presence of air, which causes it to form a dimer. The overall mass balance for each of these experiments is summarized in Table 7. The solid phase was collected by filtration at the end of the degradation experiments. The collected precipitate was weighed and then dissolved in dichloromethane and analyzed with the GC-MS. Based on the ratio of the areas of the peaks for each compound, the percentage of each compound in the solid phase is calculated as well as the moles formed. All results are reported as a percentage molar conversion of DNT. All mass balance experiments were carried out at a stir rate of 2040 rpm.

Those cases where the mass balance is more than 100 percent may be the result of an error in quantification using the standards. The standard curves for all the compounds are summarized below. The standard curves were obtained by analyzing different concentrations of the pure component on the GC and fitting the data into a linear equation.

D-1	Concentration = 9.3526*Ratio + 1.4318
D-2	Concentration = 62.209*Ratio – 0.6338
AN-1	Concentration = 9.2222*Ratio +2.4405
AN-2	Concentration = 8.5546*Ratio + 4.4682
Nitroso-1	Concentration = 161.69*Ratio + 0.8988
DAT	Concentration = 35.891*Ratio + 5.4471
DNT	Concentration = 11.643*Ratio + 2.0994

Electrochemical Reduction of TNT, RDX, and DNT With Ethanol

Effect of Applied Current

Experiments were performed at five different current settings: 23, 34, 45, 53, and 65 mA. The Honeywell UDC is capable of providing a constant current input to the electrodes. The voltage may change with a change in the ionic strength of the reaction mixture in the cathode compartment. The resistance of the aqueous solution was too high for a current higher than 65 mA so it was decided that 65 mA is the upper limit for the current range. The degradation rates observed for TNT, RDX, and DNT (with ethanol) are reported in Tables 8 through 11. Ethanol was added to the DNT solution to simulate the contaminants found in propellant wastewater.

Table 8. Experimental data for glassy carbon cathode: degradation of TNT.

Current (mA)	Stir Rate (rpm)	pH	Rate Constant (min^{-1})
23	630	8.0	0.0026
23	2040	"	0.0033
34	630	"	0.0032
34	2040	"	0.0060
45	630	"	0.0047
45	2040	"	0.0059
53	630	"	0.0053
65	630	"	0.0061
65	2040	"	0.0057
72	2040	"	0.0053
23	630	7.5	0.0040
34	630	"	0.0045
45	630	"	0.0055
53	630	"	0.0059
65	630	"	0.0052
65	2040	9.0	0.0078
53	2040	"	0.008
23	2040	"	0.0035
Note: Initial TNT at 50 mg/L and [Na_2SO_4] at 36.4 g/L.			

Table 9. Experimental data for glassy carbon cathode: degradation of RDX.

Current (mA)	Stir Rate (rpm)	pH	Rate Constant (min^{-1})
23	630	8.0	0.0010
23	2040	"	0.0012
34	630	"	0.0018
34	2040	"	0.0020
45	630	"	0.0020
45	2040	"	0.0026
53	630	"	0.0018
53	2040	"	0.0030
65	630	"	0.0017
65	2040	"	0.0030

Table 10. Experimental data for glassy carbon cathode: degradation of DNT (with ethanol).

Current (mA)	Stir Rate (rpm)	pH	Ethanol (mg/l)	Rate Constant (min^{-1})
23	630	8.0	300	0.0026
34	630	"	"	0.0036
45	630	"	"	0.0050
45	2040	"	"	0.0052
53	630	"	"	0.0056
53	2040	"	"	0.0056
65	630	"	"	0.0060
65	2040	"	"	0.0061
65	630	"	450	0.0068
65	630	"	150	0.0060
65	630	7.0	300	0.0076

Table 11. Experimental data for glassy carbon cathode: degradation of TNT in a combined mixture of TNT and RDX.

Current (mA)	Stir Rate (rpm)	pH	Rate Constant (min^{-1})
23	630	8.0	0.0036
23	2040	"	0.0045
34	630	"	0.0043
34	2040	"	0.0058
45	630	"	0.0049
45	2040	"	0.0054
53	630	"	0.0059
53	2040	"	0.0065
65	630	"	0.0062
65	2040	"	0.0061

The degradation rates for all three nitro-aromatics increased with the initial increase in the current settings but flattened out at higher currents. The behavior observed is graphically depicted in Figures 23 through 25. It can thus be concluded that the current (and hence the production of hydrogen radicals) is governing the reaction rates at smaller currents. At higher currents, however, the mass transfer limitations govern the degradation kinetics.

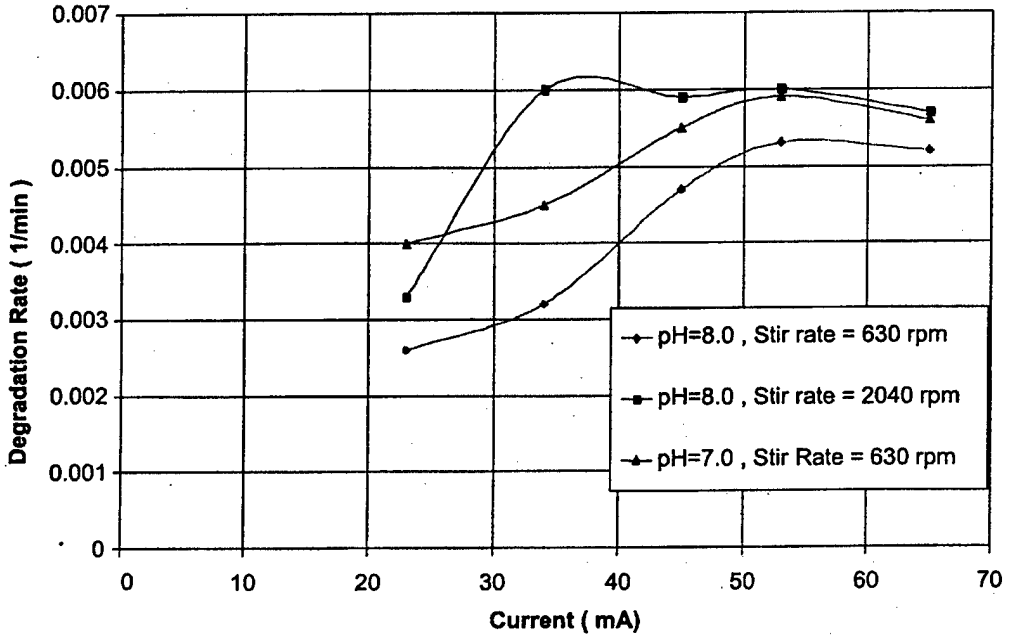

Figure 23. Degradation rates of TNT v/s Current.

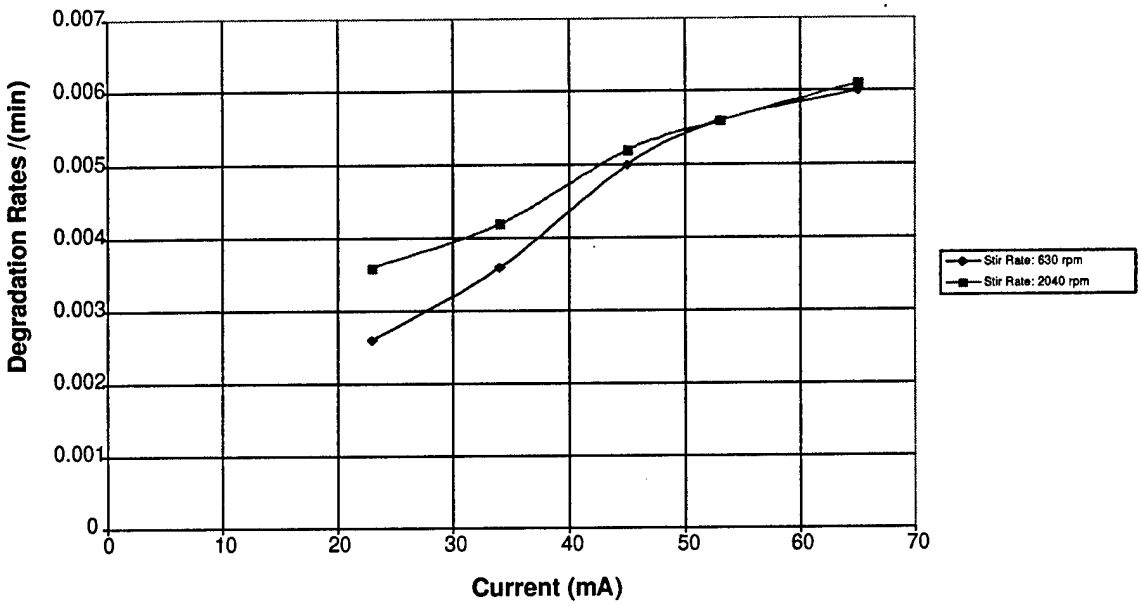

Figure 24. Degradation rates of DNT v/s Current.

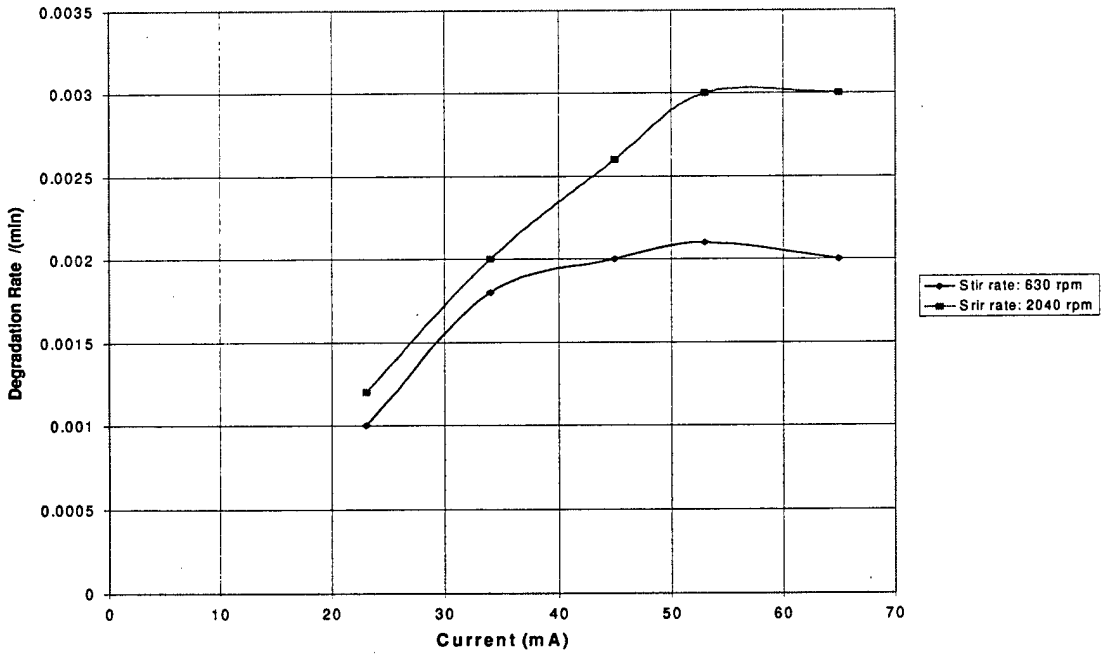

Figure 25. Degradation rates of RDX v/s Current.

Effect of Stirring Rate

Experiments were performed for given applied currents at two different speed settings of the stirrer. The stir rate in turn affects the velocity, the diffusion layer thickness, and the mixing rate in the reactor. Stir rates of 630 rpm and 2040 rpm were used. These stir rates correspond to calibration points 3 and 6 labeled on the stirrer. The rotations per minute were calculated by recording the rotation of the stir bar with a video camera and then replaying the video in slow motion while counting the rotation in each frame. With increased stirring, the degradation rates were found to increase. The increase in the stirring causes a reduction in the thickness of the diffusion layer, which allows increased transfer of nitro-aromatics from the bulk solution to the electrode surface. The degradation coefficients for different stir rate settings are presented in Tables 8 through 11.

Mass Balances for TNT

Intermediates and end-products have been identified for the degradation of TNT. An approximate 70 percent mass balance (on molar basis) was achieved for experiments conducted at two current settings. An important finding from this study is that most of the products in the experiment are present in the solid precipitate, which is formed during the degradation of TNT and which remains suspended in the reactor. The solid phase consists primarily of three types of dimers—D-1 (i.e., 2,2',6,6'-trinitro,4,4'-azoxytoluene), D-2 (i.e., 4,4',6,6'-trinitro,2,2'-azoxytoluene), and D-3 (i.e., 4,2',6,6'-trinitro,2,4'-azoxytoluene), with a minor contribution from the 2-amino-4,6-dinitrotoluene and 4-amino-2,6 dinitrotoluene. In contrast, the diaminotoluene (i.e., DAT) and 2-nitroso,4-nitrotoluene are found in the aqueous phase. It is known that some of the degradation products, such as the dimers mentioned earlier, are much less soluble in water compared to TNT, so they precipitate out of the water once their concentration increases and supersaturation occurs. Figure 9 showed the time profiles of the products.

Based on the product studies and the mass balance shown in Figure 26 and in Table 12, the importance of the relative pathways in the mechanistic scheme can be assessed for the 2,4,6 -TNT degradation shown in Figure 27.

RDX was expected to give mono-, di-, and tri-nitroso substitutes of nitro groups in RDX (commonly called MNX, DNX, and TNX respectively). An effort was made to commercially obtain these compounds, but no commercial manufacturer was found. Also, no published method of synthesis could be obtained.

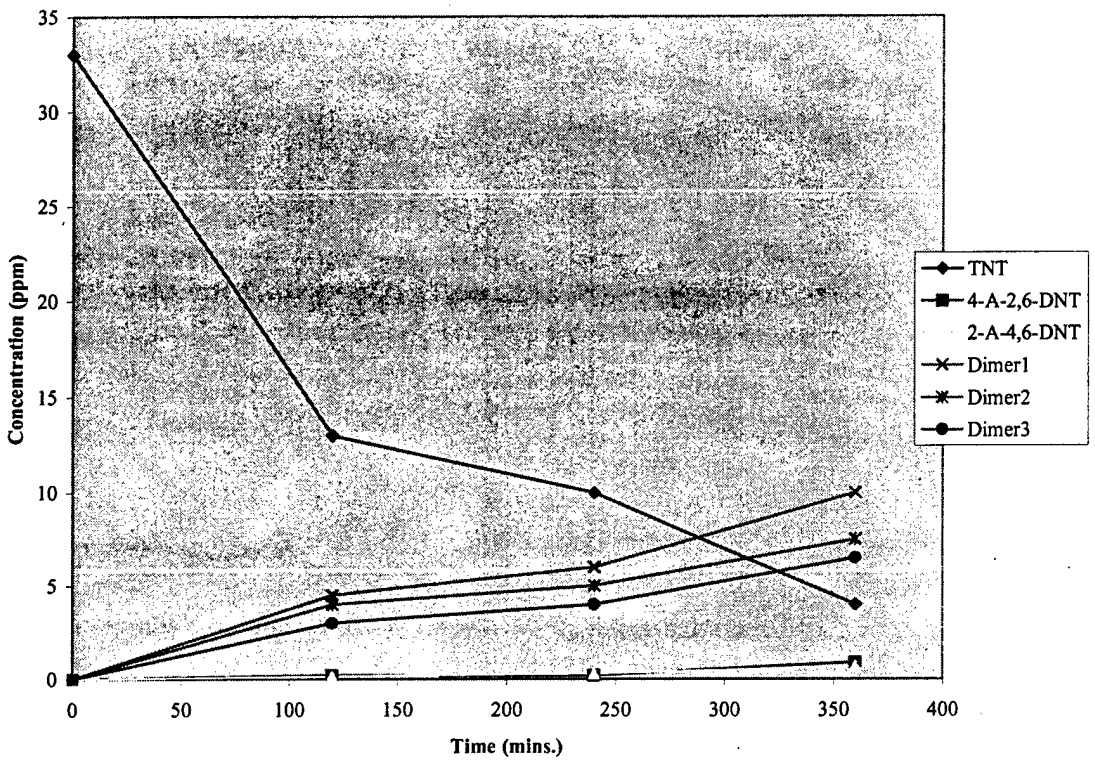

Figure 26. Product distribution of TNT (65 mA current).

Table 12. Mass balance of TNT with the glassy carbon cathode at 2040 rpm, oxygenated.

Current (mA)	Compounds	Solid Phase (% Molar Conversion of TNT to:)	Aqueous Phase (% Molar Conversion of TNT to:)
65	D-1	30.3	-
65	D-2	22.7	-
65	D-3	19.6	-
65	4-A-2,6-DNT	2.7	-
65	2-A-4,6-DNT	2.1	-
65	TNT	-	12.1
65	Total	77.4	12.1
Total Mass Balance (% Molar Conversion of TNT to identified Products) = 89.5 %			
Note: 4-A-2,6-DNT = 4-amino-2,6-dinitrotoluene; 2-A-4,6-DNT = 2-amino,4,6-dinitrotoluene; D-1 = 2,2',6,6'-trinitro,4,4'-azoxytoluene; D-2 = 4,4',6,6'-trinitro,2,2'-azoxytoluene; and D-3 = 4,2',6,6'-trinitro,2,4'-azoxytoluene.			

REDUCTION PATHWAY FOR TNT

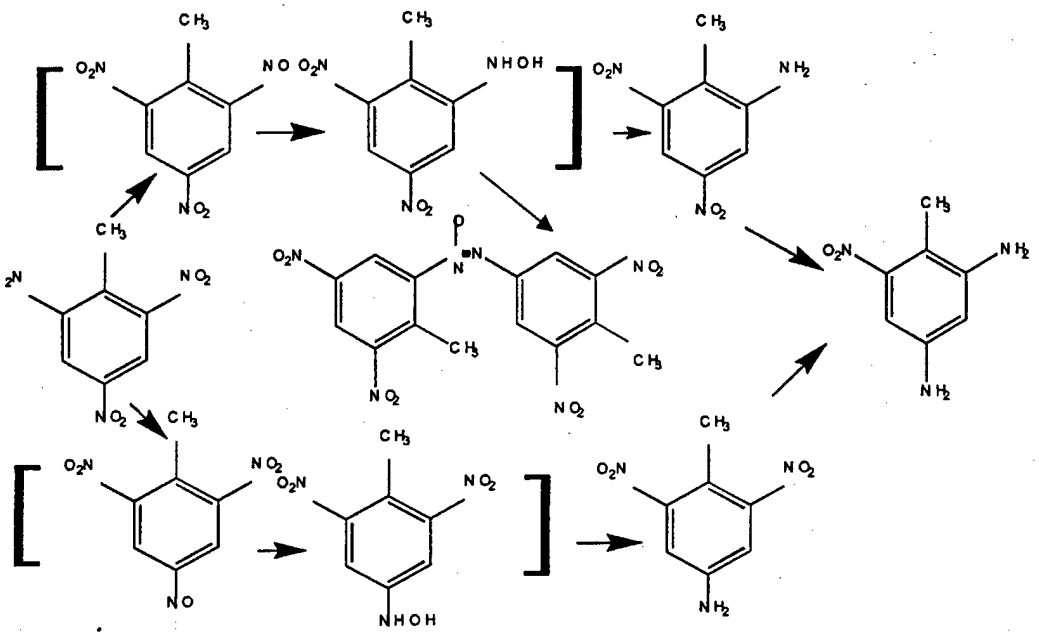

Figure 27. Proposed reduction pathway for electrochemical degradation of TNT.

4 Model Results

The model from this study is based on a similar model developed for reduction of nitrobenzene (Goodridge and Scott 1995). According to the results shown in Chapter 3, the reduction of DNT takes place through an unstable hydroxylamine intermediate, which in turn is either reduced to DAT or oxidized to a dimer. The reaction scheme is shown in Figure 28. The two secondary reactions are treated separately. On the assumption that no accumulation of the reacting species occurs and that a Tafel-type expression applies, the relation for i_A, the current density, for the primary reaction can be obtained:

$$i_A = c_A/[1/(4FkL) + 1/(k_A \exp[-b_A E'])] \quad \text{(Eq 38)}$$

Assuming:

1. The rate of diffusion of B away from the electrode is faster than the rate of the chemical reaction B→ C (i.e., as a first approximation the build up of B in the bulk of the electrolyte is negligibly small).
2. The Tafel expression can also be used for i_B, the current density, of the consecutive secondary reaction.

Let N_B be the number of kmoles of B diffusing from the surface, with $c_B \approx 0$:

$$N_B = Sk_L c_{Bs} \quad \text{(Eq 39)}$$

R_A and R_B are the number of kmoles/sec of A and B converted to B and D, respectively:

$$R_A = Sr_A \qquad \text{and} \qquad R_B = Sr_B \quad \text{(Eq 40)}$$

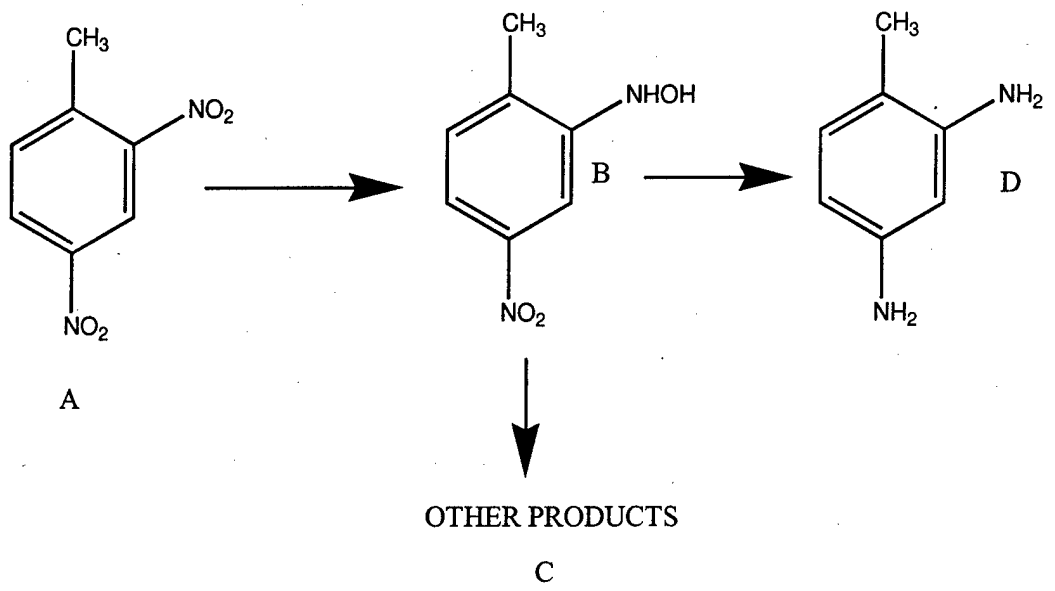

Figure 28. Reduction products of DNT.

With the previously mentioned Tafel behavior:

$$i_B = k_B c_{Bs} \exp(-b_B E') \qquad \text{(Eq 41)}$$

A colombic balance gives:

$$i_A = 4Fr_A \qquad \text{and} \qquad i_B = 8Fr_B \qquad \text{(Eq 42)}$$

Since accumulation of B at the electrode surface is negligible,

$$R_A = N_B + R_B \quad \text{or} \quad Sr_A = Sk_L c_{Bs} + Sr_B \qquad \text{(Eq 43)}$$

Giving:

$$i_A/4 = k_L c_{Bs} + i_B/8 = k_L c_{Bs} + k_B c_{Bs} \exp(-b_B E')/8 \qquad \text{(Eq 44)}$$

From Equation 44:

$$c_{Bs} = 2\, i_A/(8Fk_L + k_B \exp[-b_B E']) \qquad \text{(Eq 45)}$$

and hence

$$i_B = 2i_A\, k_B \exp[-b_B E']/(8Fk_L + k_B \exp[-b_B E']) \qquad \text{(Eq 46)}$$

Using the simple Tafel-type relationship $i_H = k_H \exp(-b_H E')$, it can be written that:

$$i = i_A + i_B + i_H \qquad \text{(Eq 47)}$$

k_A, b_A, k_H, and b_H are determined as explained previously. For the determination of k_B and b_B, the following procedure is used:

$$\frac{i_A}{i_B} = \frac{measured \quad production \quad rate \quad of \quad all \quad products}{2 * measured \quad production \quad rate \quad of \quad DAT}$$

Dividing Equation 38 by Equation 46 and simplifying arrives at:

$$\ln (i_A/i_B - ½) = \ln(4Fk_L/k_B) + b_B E' \qquad \text{(Eq 48)}$$

where E' is the stabilized potential for each of these experiments.

The kinetic parameters are:

$b_A = 0.0046\ mV^{-1}$, $k_A = 54.1$ Am/kmol

$b_B = 3.971$ 10-4 mV^{-1}, $k_B = 904$ Am/kmol

$b_H = 0.005\ mV^{-1}$, kH = 2.38 10^{-3} A/m^2

$4Fk_L = 36400$ Am/kmol; $i_{lim} = 10\ A/m^2$

The value of 4FkL is calculated using the equation $i_{lim} = nFk_L c_A^\circ$, here n = 4 and c_A° is the initial concentration of DNT.

To calculate the rate of degradation for different conditions, the following algorithm is followed:

1. All the required data such as catholyte volume (V), initial concentration (c_A°), final conversion (X_F), all the kinetic constants, cathode area (S), flow velocity (u), and current density (i) should be calculated or experimentally determined.
2. Initialize conversion (X) = 0, time = 0, count = 1.
3. Calculate $k_L = 2.0\ 10^{-4}\ u^{0.6}$.
4. Input number of integral loops (N). Calculate increment on X from $\delta X = X_F/N$.
5. Calculate E' from Equation 47, where i_A is substituted with Equation 38, i_B with Equation 46, and i_H with the Tafel Equation. This step was solved using Mathematica™ 3.0.

6. Calculate i_A from Equation 38.
7. Calculate δt from:

$$\delta t = (4FV/S)\,(c_A^{\circ}\,\delta X/i_A)$$

8. Increment X by δX, count by 1.
9. Repeat steps 5 thru 8 until count = N.

The results of the model are listed and compared with the experimental values in Tables 13 and 14.

Table 13. Comparison of experimental and model results for a glassy carbon electrode.

Current (mA)	Stir rate (rpm)	Experimental Rate Constant (min^{-1})	Model Rate Constant (min^{-1})	Model Rate Constant/ Expt Rate Constant
65	2040	0.0068	0.026	3.82
65	630	0.0053	0.026	4.9
45	2040	0.0062	0.0186	3.0
45	630	0.0048	0.0184	3.84
23	2040	0.0044	0.00978	2.22
23	630	0.0038	0.00972	2.55

Table 14. Comparison of experimental and model results for the effect of surface area.

Surface Area (cm^2)	Experimental Rate Constant (min^{-1})	Model Rate Constant (min^{-1})	Model Rate Constant/ Expt Rate Const
67.5	0.008	0.03081	3.85
57.9	0.0068	0.026	3.82
44.75	0.0049	0.0204	4.16
31.35	0.0035	0.0143	4.08
Note: All experiments conducted with glassy carbon electrode and at a current of 65mA and a stir rate of 2040 rpm.			

It can be observed from the model results that the model overestimates the rate constant by as much as a factor of four in some cases. This may be attributed to the fact that the kinetic parameters were estimated using a clean electrode, which, in fact, is one of the assumptions of the model. In the course of an experiment, however, there seems to be a heavy deposit of inert products such as dimers and salt on the surface of the electrode. Thus, the overestimation of the rate constant may be due to deposition of some solids on the surface of the electrode. This conclusion can also be supported by the fact that the model results are much closer to the experimental results at lower currents where dimer formation is lower.

This result has to be verified by carrying out additional experiments in which the surface of the electrode is periodically cleaned. If the reaction rate does not increase after that, then the exact mass transfer coefficient must be determined

experimentally instead of using the empirical formula. Moreover, the model results show that the reaction rate is still charge-transfer-controlled, whereas the experimental results show that the reaction rate is more mass-transfer-limited, especially for higher currents. This also suggests that there might be a solid deposition on the surface of the electrode.

5 Discussion

The research shows that electrochemical reduction of the three nitro-aromatics 2,4,6-TNT, 2,4-DNT, and RDX is taking place readily in the reactor. The rates of degradation observed for TNT and DNT are almost similar, while the degradation rates of RDX are much slower under the applied conditions. The degradation rates of DNT with added ethanol are almost similar to the rates observed with DNT alone. In the experiments that combined both RDX and TNT with the solution, the degradation rates of TNT were unaffected by the presence of RDX. The products of electrochemical reduction of TNT were three kinds of dimers and various amino-substitutes of the nitro groups. The products of the electrochemical degradation of DNT are primarily 2,4-DAT and a mixture dominated with the azoxy dimers. In oxygenated systems, a large portion of the products is present in the form of precipitate rather than in the aqueous phase.

The two factors that have the most significant effect on the degradation rates among the various parameters analyzed are: stirring rate and current density. Change in the pH does alter the degradation kinetics, but the effect is not as prominent as the above two factors. Moreover, alteration of the effluent stream pH by addition of chemicals may not be a good option — it may increase the operational cost significantly. The available surface area of the cathode has a linear effect on the rate of degradation of 2,4-DNT. Among the two aforementioned controlling factors, the stirring rate determines the mass transfer rate and the current density determines both the intrinsic chemical rate and the mass transfer (an explanation follows).

The kinetics in an electrochemical system can be explained to a great extent by a diffusion layer theory (Scott 1991). The reactions that are going on in the cathodic solution can be written as follows:

$$2H^+ + 2e \rightarrow 2H \qquad \text{(R-1)}$$

$$C_7H_5N_2O_4NO_2 + 2H \rightarrow C_7H_5N_2O_4NO + H_2O \qquad \text{(R-2)}$$

$$C_7H_5N_2O_4NO + 2H \rightarrow C_7H_5N_2O_4NHOH \qquad \text{(R-3)}$$

$$C_7H_5N_2O_4NHOH + 2H \rightarrow C_7H_5N_2O_4NH_2 + H_2O \quad \text{(R-4)}$$

$$2H \rightarrow H_2 \quad \text{(R-5)}$$

The reactor solution is completely mixed in the bulk. Because of the solid–liquid interface, convective mixing does not take place at the cathode surface; therefore, the protons from the bulk move to the cathode surface (to undergo reaction R-1) by diffusing from the bulk to the surface. The opposite happens with the hydrogen radicals, which are extremely reactive. Besides undergoing the reactions R-2, R-3, and R-4 that result in the degradation of the nitro-aromatic, hydrogen radicals readily combine with each other to form hydrogen gas (reaction R-5). Thus the nitro-aromatic has to move through the diffusion layer formed by the protons and hydrogen radicals to undergo the reduction reaction.

The stirring in the solution (or agitation by other means) determines the mixing in the bulk in the vicinity of the cathode. This mixing in turn determines the diffusion layer thickness. Higher stirring or agitation results in a smaller diffusion layer thickness. The smaller the diffusion layer, the faster the nitro-aromatic would move toward the electrode and, therefore, the higher the degradation rate would be.

Similar reasoning can be applied to the current density. An increase in current causes more rapid release of electrons (or a more rapid conversion of H+ to H), which means a steeper concentration gradient of protons from the bulk to the electrode surface. This concentration would in turn lead to a lower proton concentration in the diffusion layer, which would again yield higher transfer rates of nitro-aromatics and hence higher degradation rates.

As was previously discussed and is shown in Figures 23 through 25, the mass transfer limitation starts to affect the degradation kinetics at higher currents. Additional experiments were performed with improved hydrodynamics to try and overcome these limitations. One of the ways in which the diffusion layer thickness could be reduced is a recycle, with water flowing over the cathode. Thus a reactor was operated as shown in the schematic in Figure 29. The reactor solution was released from the bottom and pumped up again to fall over the cathode. This procedure increased the degradation rate tremendously as compared to the rate observed without this recycle. The two reactor results are compared in Figure 30. This result also ascertained that it was indeed mass transfer that was limiting at higher currents.

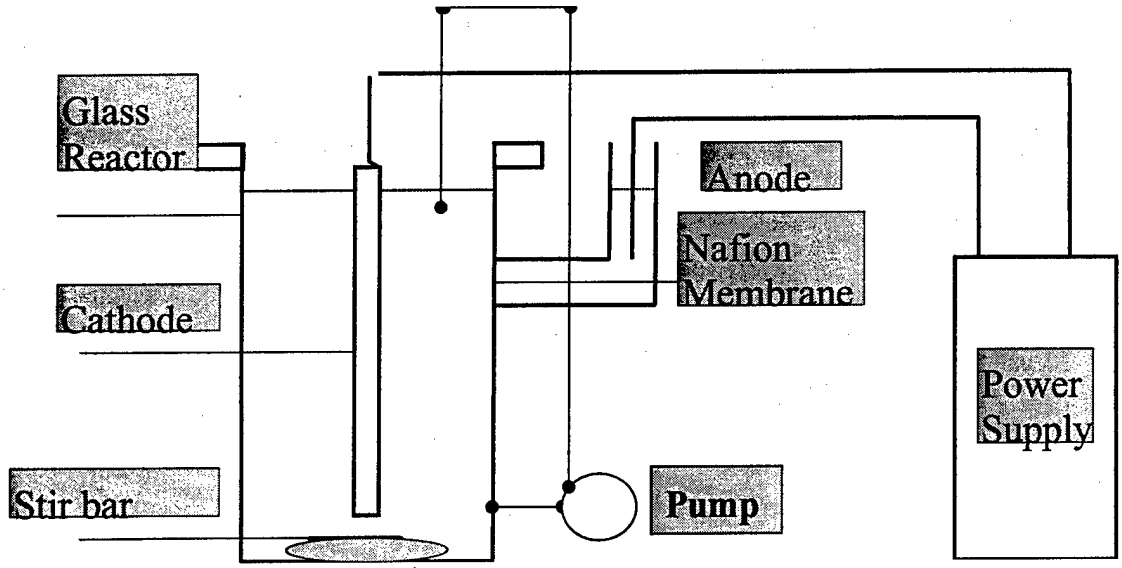

Figure 29. Experimental setup for the recycled flow experiments.

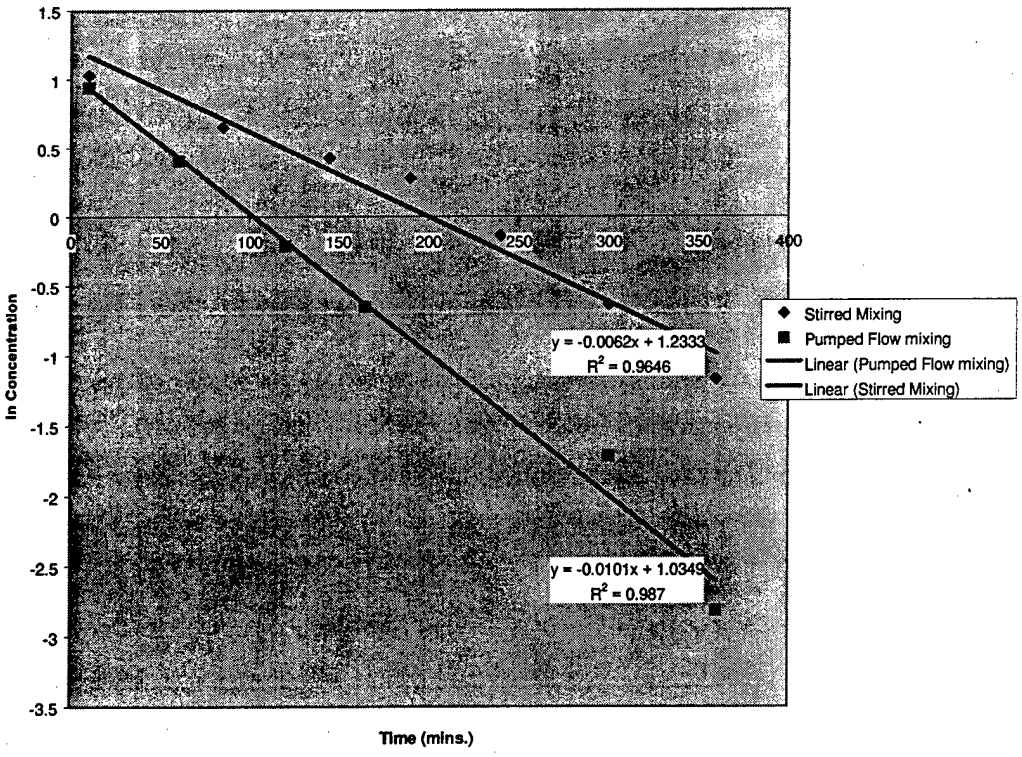

Figure 30. Comparison of degradation rates for batch and recycled flow reactor.

6 Conclusions

The transformation of two nitro-aromatics (DNT and TNT) to their corresponding reduced by-products has been shown to occur through purely abiotic mechanisms induced by electric current.

DNT transformation in the absence of oxygen primarily yields DAT. However, when oxygen is present, the reduced compound or its partially reduced by-products can polymerize to form dimers, which precipitate from solution. These are azoxy dimers with nitro groups remaining. TNT also appears to form dimers; however, the absence of analytical standards or published synthesis techniques has made their identification questionable at this point.

The reaction appears to be mass transfer limited, indicating the need to produce flow patterns in any reactor to mix the reactants rather than relying on diffusion. Mathematical modeling indicates that the rate predicted from initial kinetic parameters far exceeds the rates observed over longer periods of treatment. This observation suggests that some materials are depositing on the surface of the electrodes, which should also be addressed in terms of removal by cleaning or turbulence in the system.

References

Cited

Barrows, S.E., C.J. Cramer, D.G. Truhlar, M.S. Elovitz, and E.J. Weber, "Factors Controlling Regioselectivity in the Reduction of Polyaromatics in Aqueous Solution," *Environ. Sci. Technol.*, 30(1996)3028-3038.

Bausum, H.T., W.R. Mitchell, and M.A. Major, "Biodegradation of 2,4- and 2,6-Dinitrotoluene by Freshwater Microorganisms," *J. Environ. Sci. Health*, A27(3)(1992)663-695.

Beard, R.R., and J.T. Noe, "Anaerobic Nitro and Amino Compounds," in G.D. Clayton and F.E. Clayton, eds, *Patty's Industrial Hygiene and Toxicology*, Vol. 2A (John Wiley and Sons, New York, 3rd ed., 1981).

Berchtold, S.R., S.L. VanderLoop, M.T. Suidan, and S.W. Maloney, "Treatment of 2,4-Dinitrotoluene Using a Two-stage System: Fluidized-bed Anaerobic Granular Activated Carbon Reactors and Aerobic Activated Sludge Reactors," *Wat. Environ. Res.*, 67(1995) 1081-1091.

Boopathy R., M. Wilson, and C.F. Kulpa, "Anaerobic Removal of TNT Under Different Electron Accepting Conditions: Lab Study," *Water Environ. Res.*, 65(1993)271-275.

Bowyer, W.J., and D.H. Evans, "Electrochemical Reduction of Vicinal Dinitro Compounds," *J. Org. Chem.*, 53(1988)5234-5239.

Eisenberg, M., C.W. Tobias, and C.R. Wilke, "Ionic Mass Transfer and Concentration Polarization at Rotating Electrodes," *J. Electrochemical Soc.*, v101(1954)306-320.

Fisher, R.H., and J.M. Taylor, *Munitions and Explosive Wastes* (Noyes Data Corporation, Park Ridge, NJ, 1983), pp 297-303.

Fry, A.J., "Electrochemistry of Nitro Compounds," in *The Chemistry of Amino, Nitroso, and Nitro Compounds and Their Derivatives*, S. Patai, Ed., Vol 1 (Wiley-Interscience, Chichester, 1982), pp 319-337.

Goodridge, F., and K. Scott, *Electrochemical Process Engineering, A Guide to the Design of Electrolytic Plant* (Plenum Press, New York, 1995).

Haidour, A., and J.L. Ramos, "Identification of Products Resulting From the Biological Reduction of TNT and DNT by Pseudomonas sp.", *Environ. Sci. Technol.*, 30(1996)2365-2370.

Ho, P.C., and C.S. Daw, "Adsorption and Desorption of Dinitrotoluene on Activated Carbon," *Environ.Sci.Tech.*, 22(1988)919-24.

Hughes, J.B., C. Wang, K. Yesland, A. Richardson, R. Bhadra, G. Bennett, and F. Rudolph, "Bamberger Rearrangement During TNT Metabolism by C. acetobutylicum," *Environ. Sci. Tech.*, 32(1998)494-500.

Janssen, H.J., A.J. Kruithof, G.J. Steghuis, and K.R. Westerterp, "Kinetics of the Catalytic Hydrogenation of 2,4-Dintrotoluene. 1. Experiments, Reaction Scheme and Catalyst Activity," *Ind. Eng. Chem. Res.*, 29(1990)754-766.

Jenkins, T., and M. Walsh, "Field Screening Methods for Munitions Residues in Soils, Semiarid Technologies for Remediating Sites Contaminated with Explosive and Radioactive Waste," EPA/625/K-93/001 (Office of Research and Development, Washington, DC, 1993).

Kitts, C.L., D.P. Cunningham, and P.J. Unkefer, "Isolation of Three Hexahydro-1,3,5-trinitro-1,3,5-triazine-degrading Species of the Family *Enterobacteriaceae* from Nitramine Explosive Contaminated Soil," *Appl. Environ. Microbiol.*, v60(1994)4608-4611.

Kline C. Kline Guide to the U.S. Chemical Industry, 5th ed. (Kline and Company, Inc., Fairfield, NJ, 1990), pp 106-109.

Kopilov, J., and D.H. Evans, "Electrochemical Reduction of Some a-Haloacetanilides," *J. Electroanal. Chem.*, 280(1990)435-438.

Laviron, E., and A. Vallat, "Thin Layer Linear Sweep Voltammetry: A Study of the Condensation of Nitrosobenzene With Phenylhydroxylamine, *J. Electroanal. Chem. Interfacial Electrochem.*, 46(1973)421-6.

Martigny, P., and J. Simonet, "On the Existence of the Intermediate Nitroso During the Mixed Electrochemical Reduction of Nitro Compounds and Organic Halides," *J. Electroanal. Chem.*, 148(1983)51-60.

McCormick, N.G., J.H. Cornell, and A.M. Kaplan, "Identification of biotransformation products from 2,4-Dinitrotoluene," *Appl. Environ. Microbiol.*, 35(1978)945-948.

McCormick, N.G., J.H. Cornell, and A.M. Kaplan, "Biodegradation of Hexahydro-1,3,5-trinitro-1,3,5-triazine," *Appl. Environ. Microbiol.*, v42(1981)817-823.

Neri, G., Maria G. Musolino, Candida Milone, and Signorino Galvagno. "Kinetic Modeling of 2,4-Dinitotoluene Hydrogenation over Pd/C," *Ind. Eng. Chem. Res.*, 34(1995)2226-2231.

Noguera, D.R., and D.I. Freedman, "Reduction and Acetylation of 2,4-Dinitrotoluene by a Pseudomonas aeruginosa Strain," *Appl. Environ. Microbiol.*, 62(7)(1996)2257-2263.

Parrish, F.W., "Fungal Transformation of 2,4-Dinitrotoluene and 2,4,6-Trinitrotoluene," *Appl. Environ. Micro. Biol.*, 47(1977)1295-98.

Ruhl, J.C., D.H. Evans, P. Hapiot, and P. Neta, "Fast Cleavage Reactions Following Electron Transfer. Fast Reduction of 1,1-Dinitrocyclohexane," *J. Am. Chem. Soc.*, 113(1991)5188-5194.

Ruhl, J.C., D.H. Evans, and P. Neta, "Electrochemical Reduction of Some a-Substituted Nitroalkanes," *J. Electroanal. Chem.*, 340(1992)257-272.

Sandler, S.R., and W. Karo, *Organic Functional Group Preparations*, Vol. 2 (Academic Press: London, 1971).

Sax, N.I., and R.J. Lewis, *Dangerous Properties of Industrial Materials*, 7th Ed, Vol.2, 3 (Von Nostrand Reinhold, New York, 1989).

Schackmann, A., and R. Muller, "Reduction of nitro-aromatic compounds by different species under aerobic conditions," *Appl. Microbiol. and Biotechnol.*, 34(1991)809-813.

Schmelling, D.C., and K.A. Gray, "Photocatalytic Transformation and Mineralization of TNT in TiO_2 Slurries," *Water Research*, 29(1995)2651-2662.

Schmelling, D.C., K.A. Gray, and P.V. Kamat, "Role of Reduction in the Photocatalytic Degradation of TNT," *Env. Sci. & Tech.*, v30(1996)2547-2555.

Scott, K., *Electrochemical Reaction Engineering* (Academic Press, London, 1991).

Shindo, H., and C. Nishihara, "Detection of Nitrosobenzene as an Intermediate in the Electrochemical Reduction of Nitrobenzene on Ag in a Flow Reactor," *J. Electroanal. Chem.*, 263(1989)415-20.

Spanggord, R.J., J.C. Spain, S.F. Nishino, and K.E. Mortelmans, "Biodegradation of 2,4-Dinitrotoluene by a Pseudomonas sp.," *Appl. Environ. Microbiol.*, 57(1991)3200-3205.

Terpko, M.O., and R.F. Heck, "Palladium-catalyzed Triethylammonium Formate Reductions. 3. Selective Rreduction of Dinitroaromatic Compounds," *J. Org. Chem.*, 45(1980)4992-4993.

Tri-Service Reliance Joint Engineers–Environmental Quality Technical Area Panel, Tri-service Environmental Quality Strategic Plan Program, Draft Program User Review, Fort Belvoir, VA (1992).

Valli, K., B.J. Brock, D.K. Joshi, and M.H. Gold, "Degradation of 2,4-Dinitrotoluene by the Lignin-degrading Fungus Phanerochaete chrysosporium," *Appl. Environ. Microbiol.*, 58(1)(1992)221-228.

Young, D.M., C.L. Kitts, P.J. Unkefer, and K.L. Ogden, "Biological Breakdown of RDX in Slurry Reactors," *Biotechnol. Bioeng.*, 56(1997)258-267.

Uncited

Agrawal, A., and P.G. Tratnyek, "Reduction of Nitro aromatic Compounds by Zero-valent Iron Metal," *Environ. Sci. Technol.* 30(1996)153-160.

Benedetti, A., G. Fagherazzi, F. Pinna, and M. Selva, "The Influence of a Second Metal Component (Cu, Sn, Fe) on Pd/ SiO_2 Activity in the Hydrogenation of 2,4-Dinitrotoluene," *Catal.Lett*, 10(1991)215-224.

Bird, A.J., D.T. Noble Thompson, "Metal Catalysis in Industrial Hydrogenation, PartI: Palladium Solubility and Hydrogen Availability," In *Catalysis in Organic Synthesis,* Seventh Conference, Jones, W.H., ed (Academic Press, New York, 1980).

Burge, H.D., D.J. Collins, and B.H. Davis, "Intermediates in the Raney Nickel Catalyzed Hydrogenation of Nitrobenzene to Aniline," *Ind. Eng. Chem. Prod. Res. Dev.,* 19(1980)389-391.

Burton, D.T., S.D. Turley, and G.T. Peters, "Toxicity of RDX to the Freshwater Green Alga," *Water, Air and Soil Pollution,* 76(1994)449-457.

Chang, J., *Anaerobic Biotransformation of 2,4-Dinitrotoluene with Different Primary Substrates,"* Doctoral Dissertation (University of Cincinnati, 1996).

Dalmargo, J., R.A. Yunes, and E.L. Simionatto, "Mechanism of Reaction of Azobenzene Formation From Aniline and Nitrosobenzene in Basic Conditions: General base catalysis by hydroxide ion," *J. Phys. Org. Chem.,* 7(1994)399-402.

Dovell, F.S., W.E. Ferguson, and H. Greenfield, "Kinetic Study of Hydrogenation of Dinitrotoluene and m-Dinitrobenzene". *Ind.Eng.Chem.Prod.Res.Dev,* 9(1970)224.

Eastern Research Group, Inc., "Introduction. Approaches for the remediation of federal facility sites contaminated with explosive or radioactive wastes," EPA/625/R-93/013, 1993.

Haber, F., *Z. Elektrochem,* 22(1898)506.

Hallas, L.E., and M. Alexander, "Microbial Transformation of Nitro-aromatic Compounds in Sewage Effluent," *Appl. Environ. Microbiol,* 45(1983)1234-1241.

Jolas, J., "Electrochemical Degradation of 2,4-Dinitrotoluene," Masters Thesis (The University of Cincinnati, 1997).

Kaplan, D.L., and A.M. Kaplan, "Mutagenecity of 2,4,6-trinitrotoluene Surfactant Complexes," *Bull. Environ. Contam. Toxicol.,* 28(1982)33.

Keither, L.H., and W.A. Telliard, "Priority pollutants - A perspective view," *Enviro. Sci. Technol.,* 13(1979)416-423.

Lessard, J., and A.Velin-Prikidanovics, "An Efficient Electrosynthesis of 2,4- and 2,6-Diaminotoluenes," *J. Appl. Electrochem,* 20(1990)527-29.

Li, L., E.F. Glyna, and J.E. Sawicki, Treatability of DNT Process Wastewater by Supercritical Water Oxidation, *Wat. Environ. Res.,* 65(1993)250-2577.

Liu, D., K. Thompson, and A.C. Anderson, "Identification of Nitroso Compounds from Biotransformation of 2,4-Dinitrotoluene," *Appl. Environ. Micro. Biol.,* 47(1984)1295-1298.

Maloney, S.W., M.T. Suidan, and S.A. Berchtold, "Treatment of Propellant Production Wastewater Containing DNT Using Expanded-bed Granular Activated Carbon Anaerobic Reactors, *Proceedings of the 16th Army Environmental Symposium* (Williamsburg, VA, June 1992).

Newman, J.S., *Electrochemical Systems*, 2nd ed (Prentice Hall, NJ, 1991).

Noguera, D.R., and D.I. Freedman, "Characterization of Products from the Biotransformation of 2,4-dinitrotoluene by Denitrifying Enrichment Cultures, *Wat. Environ. Res.,* 69(3)(1997)260-268.

Patai, S., *The Chemistry of Amino, Nitroso and Nitro Compounds and Their Derivatives,* 1st Ed. (Wiley InterScience, Chichester, 1982).

Pizzolatti, M.G., and R.A. Yunes, "Azoxybenzene Formation from Nitrosobenzene and Phenylhydroxylamine: A unified view of the catalysis and mechanisms of the reactions, *J. Chem. Soc. Perkin Trans. II* (1990)759-64.

Peters, G.T., D.T. Burton, R.L. Paulson, and S.D. Turley, "Toxicity of RDX to invertebrates," *Environ. Toxicol. Chem.,* 10(1991)1073.

Sakakibara, Joseph, R.V. Flora, Makram T. Suidan, Pratim Biswas, and Masao Kuroda, "Measurements of Mass Transfer Coefficients with an Electrochemical Method using Dilute Electrolyte Solution," *Wat.Res.,* 1(1994)9-16.

Sakakibara, Joseph, R.V. Flora, Makram T. Suidan, and Masao Kuroda, "Modeling of Electrochemically activated Denitrifying Biofilms," *Wat. Res.,* 28(1994)1077-86.

Schmelling, D.C., and K.A. Gray, "Photocatalytic Transformation and Mineralization of TNT in TiO_2 Slurries," *Water Research,* 29(1995)2651-2662.

Shindo, H., and C. Nishihara, "Detection of Nitrosobenzene as an Intermediate in the Electrochemical Reduction of Nitrobenzene on Ag in a flow reactor," *J. Electroanal. Chem.,* 263(1989)415-20.

Suh, D.J., T.J. Park, and S. Ihm, "Characteristics of Carbon Supported Palladium Catalysts for Liquid-Phase Hydrogenation of Nitro-aromatics," *Ind. Eng. Chem. Res.*, 31(1992)1849.

Sulfita, J.M., A. Horowitz, D.R. Shelton, and J.M. Tiedje, "Dehalogenation: A Novel Pathway for Anaerobic Biodegradation of Haloaromatic Compounds, *Science,* 218(1982)1115-1117.

Udupa, H.V.K., *Indian J. Chem. Eng.,* 30(1988)53.

Yao, H.-C., and P.H. Emmett, "Kinetics of Liquid Phase Hydrogenation, IV. Hydrogenation of Nitrocompounds over Raney Nickel and Nickel Powder Catalysts," *J. Am. Chem. Soc.* 84(1962)1086-1091.

Young, D.M., C.L. Kitts, P.J. Unkefer, and K.L. Ogden, "Biological Breakdown of RDX in Slurry Reactors," *Biotechnol. Bioeng.* 56(1997)258-267.

CERL Distribution

Chief of Engineers
ATTN: CEHEC-IM-LH (2)
ATTN: HECSA Mailroom (2)
ATTN: CECC-R
ATTN: CERD-L
ATTN: CERD-M

Industrial Operations Command
ATTN: AMSIO-EQC

US Army Materiel Command (AMC)
Alexandria, VA 22333-0001
ATTN: AMCEN-F
Installations:
Rock Island, IL 61299-7190
ATTN: AMXEN-C
Radford Army Ammunition Plant
ATTN: SMCRA-EN 24141
Aberdeen Proving Ground
ATTN: STEAP-FE 21005
Rock Island Arsenal 61299
ATTN: SMCRI-PW
Harry Diamond Lab
ATTN: Library 20783
Picatinny Arsenal 07806
ATTN: AMSTA-AR-IMC

US Army Materials Tech Lab
ATTN: SLCMT-DPW 02172

US Army Environmental Center
ATTN: SFIM-AEC-NR 21010
ATTN: SFIM-AEC-CR 64152
ATTN: SFIM-AEC-SR 30335-6801
ATTN: AFIM-AEC-WR 80022-2108

Defense Tech Info Center 22304
ATTN: DTIC-O (2)

22
8/99

REPORT DOCUMENTATION PAGE

Form Approved
OMB No. 0704-0188

1. AGENCY USE ONLY (Leave Blank)	2. REPORT DATE	3. REPORT TYPE AND DATES COVERED
	October 1999	Final

4. TITLE AND SUBTITLE
Electrochemical Reduction of Nitro-Aromatic Compounds: Product Studies and Mathematical Modeling

5. FUNDING NUMBERS
62720
D048
U08/09

6. AUTHOR(S)
Devakumaran Meenakshisundaram, Manish Mehta, Simo Pehkonen, and Stephen W. Maloney

7. PERFORMING ORGANIZATION NAME(S) AND ADDRESS(ES)
U.S. Army Construction Engineering Research Laboratory (CERL)
P.O. Box 9005
Champaign, IL 61826-9005

8. PEFORMING ORGANIZATION REPORT NUMBER
TR 99/85

9. SPONSORING / MONITORING AGENCY NAME(S) AND ADDRESS(ES)
Headquarters, U.S. Army Corps of Engineers (HQUSACE)
20 Massachusetts Avenue, NW.
Washington, DC 20314-1000

10. SPONSORING / MONITORING AGENCY REPORT NUMBER

9. SUPPLEMENTARY NOTES
Copies are available from the National Technical Information Service, 5385 Port Royal Road, Springfield, VA 22161

12a. DISTRIBUTION / AVAILABILITY STATEMENT
Approved for public release; distribution is unlimited.

12b. DISTRIBUTION CODE

13. ABSTRACT *(Maximum 200 words)*

Nitro-aromatics: 2,4,6-trinitrotoluene (TNT), 2,4-dinitrotoluene (DNT) and hexa-hydro-1,3,5– trinitro- triazine (RDX) are the major constituents of wastewaters discharged from propellant and explosive manufacturing units and munitions load, assembly, and pack operations. More than 1,200 current and former U.S. Department of Defense and U.S. Department of Energy facilities have problems with explosive contamination.

The objective of this project was to study the electrochemical degradation of nitro-aromatic compounds under various conditions to enable the formulation of a mathematical model and to design a plug flow reactor for the same. The transformation of DNT and TNT to their corresponding reduced by-products has been shown to occur through purely abiotic mechanicsms induced by electric current.

14. SUBJECT TERMS
Nitro-aromatics
Munitions waste disposal
Electrochemical degradation
hazardous waste management
chemical pollutants
TNT, DNT, RDX

15. NUMBER OF PAGES
70

16. PRICE CODE

17. SECURITY CLASSIFICATION OF REPORT	18. SECURITY CLASSIFICATION OF THIS PAGE	19. SECURITY CLASSIFICATION OF ASTRACT	20. LIMITATION OF ABSTRACT
Unclassified	Unclassified	Unclassified	SAR